Journal of Hyperbolic Differential Equations
Vol. 3, No. 3 (2006) 529–559

ENTROPY STABLE APPROXIMATIONS OF NAVIER–STOKES EQUATIONS WITH NO ARTIFICIAL NUMERICAL VISCOSITY

EITAN TADMOR

Department of Mathematics
Center for Scientific Computation and Mathematical Modeling (CSCAMM)
and Institute for Physical Science and Technology (IPST)
University of Maryland, MD 20742, USA
tadmor@cscamm.umd.edu

WEIGANG ZHONG

Department of Mathematics
and Center for Scientific Computation and Mathematical Modelling (CSCAMM)
University of Maryland, College Park, MD 20742
wzhong@math.umd.edu

Received 4 Dec. 2005
Accepted 28 Dec. 2005

Communicated by the Editors

Dedicated with appreciation to Tai-Ping Liu on his 60th birthday

Abstract. We construct a new family of entropy stable difference schemes which retain the *precise* entropy decay of the Navier–Stokes equations,

$$d/dt \int_x (-\rho S)dx = -\int_x ((\lambda + 2\mu)q_x^2/\theta + \kappa(\theta_x/\theta)^2)dx.$$

To this end we employ the entropy conservative differences of [24] to discretize Euler convective fluxes, and centered differences to discretize the dissipative fluxes of viscosity and heat conduction. The resulting difference schemes contain no artificial numerical viscosity in the sense that their entropy dissipation is dictated solely by viscous and heat fluxes. Numerical experiments provide a remarkable evidence for the different roles of viscosity and heat conduction in forming sharp monotone profiles in the immediate neighborhoods of shocks and contacts.

Keywords: Navier–Stokes equations; viscosity; heat conduction; entropy decay; entropy variables; difference schemes; entropy conservative schemes; entropy stability.

Mathematics Subject Classification 2000: 76N10, 65M12

1. Introduction

We consider the full Navier–Stokes (NS) equations for compressible viscous flows in one-space dimension,

$$\frac{\partial}{\partial t}\begin{bmatrix}\rho\\ m\\ E\end{bmatrix}+\frac{\partial}{\partial x}\begin{bmatrix}m\\ qm+p\\ q(E+p)\end{bmatrix}=(\lambda+2\mu)\frac{\partial^2}{\partial x^2}\begin{bmatrix}0\\ q\\ q^2/2\end{bmatrix}+\kappa\frac{\partial^2}{\partial x^2}\begin{bmatrix}0\\ 0\\ \theta\end{bmatrix}. \qquad (1.1)$$

Here, $\rho=\rho(x,t)$ is the density of the flow, $m=m(x,t)$ is the momentum and $E=E(x,t)$ stands for the total energy per unit volume. The three equations express, respectively, conservation laws of mass, momentum and total energy for the flow, driven by convective fluxes on the left together with viscous and heat fluxes on the right. These fluxes involve the velocity $q:=m/\rho$, the pressure $p=p(x,t)$ which is determined by an ideal polytropic equation of state,

$$p=(\gamma-1)e,\quad e:=E-\frac{m^2}{2\rho}, \qquad (1.2)$$

and the absolute temperature, $\theta=\theta(x,t)>0$, such that $C_v\rho\theta=e$. The constant $\gamma>1$ is the specific heat ratio and $e=e(x,t)$ is the internal energy. On the right-hand side of (1.1), we have the viscous and heat fluxes, depending on the constant Lamé coefficients of the viscosity $\lambda,\mu>0$ and the constant conductivity $\kappa>0$. Finally, $C_v>0$ is the specific heat at constant volume; for simplicity, we set $C_v=1$ while rescaling $\kappa\mapsto\kappa/C_v$.

If the heat flux is excluded from the full NS equations, i.e. $\kappa=0$, we obtain the viscous NS equations

$$\frac{\partial}{\partial t}\begin{bmatrix}\rho\\ m\\ E\end{bmatrix}+\frac{\partial}{\partial x}\begin{bmatrix}m\\ qm+p\\ q(E+p)\end{bmatrix}=(\lambda+2\mu)\frac{\partial^2}{\partial x^2}\begin{bmatrix}0\\ q\\ q^2/2\end{bmatrix}. \qquad (1.3)$$

On the other hand, if we turn off the viscosity, i.e. $\lambda=\mu=0$, then the NS equations amount to

$$\frac{\partial}{\partial t}\begin{bmatrix}\rho\\ m\\ E\end{bmatrix}+\frac{\partial}{\partial x}\begin{bmatrix}m\\ qm+p\\ q(E+p)\end{bmatrix}=\kappa\frac{\partial^2}{\partial x^2}\begin{bmatrix}0\\ 0\\ \theta\end{bmatrix}. \qquad (1.4)$$

If the heat flux and viscosity are both taken away, the system (1.1) is reduced to the compressible Euler equations,

$$\frac{\partial}{\partial t}\begin{bmatrix}\rho\\ m\\ E\end{bmatrix}+\frac{\partial}{\partial x}\begin{bmatrix}m\\ qm+p\\ q(E+p)\end{bmatrix}=0. \qquad (1.5)$$

The additional viscous and heat flux terms on the right-hand side of the various NS equations (1.1), (1.3) or (1.4), are dissipative terms in the sense that they are responsible for the dissipation of the total *entropy*. To this end, we now discuss the entropy balance associated with the above equations. We begin with the specific entropy $S := \ln(p\rho^{-\gamma})$. A straightforward manipulation on (1.1), (1.2) yields the transport equation,

$$S_t + qS_x = \frac{\kappa}{\rho}(\ln\theta)_{xx} + (\lambda+2\mu)\frac{q_x^2}{e} + \frac{\kappa}{\rho}\left(\frac{\theta_x}{\theta}\right)^2. \tag{1.6}$$

Multiplied by ρ, (1.6) becomes

$$\rho S_t + mS_x = \kappa(\ln\theta)_{xx} + (\lambda+2\mu)\frac{q_x^2}{\theta} + \kappa\left(\frac{\theta_x}{\theta}\right)^2. \tag{1.7}$$

On the other hand, pre-multiplying the continuity equation, $\rho_t + m_x = 0$, by S and adding it to (1.7),

$$\frac{\partial}{\partial t}(-\rho S) + \frac{\partial}{\partial x}\big(-mS + \kappa(\ln\theta)_x\big) = -(\lambda+2\mu)\frac{q_x^2}{\theta} - \kappa\left(\frac{\theta_x}{\theta}\right)^2. \tag{1.8}$$

Spatial integration of (1.8) then yields

$$\frac{d}{dt}\int_x (-\rho S)\,dx = -(\lambda+2\mu)\int_x q_x^2\cdot\frac{1}{\theta}\,dx - \kappa\int_x \theta_x^2\left(\frac{1}{\theta}\right)^2 dx. \tag{1.9}$$

Since the expression on the right is negative, we conclude that the total entropy, $\int_x(-\rho S)\,dx$, is decreasing in time, thus recovering the second law of thermodynamics, e.g. [4]. In fact, Eq. (1.9) specifies the precise entropy decay rate, which is dictated by the viscous and heat fluxes through their dependence on the nonnegative κ, λ, and μ.

The purpose of this paper is to present a systematic study of difference schemes which respect the above entropy dissipation statements. The typical approach by practitioners in the field of Computational Fluid Dynamics is to address the general issue of entropy stability by adding "enough" artificial numerical viscosity — often an excessive amount of it, in order to mask various discretizations errors and enforce the decay of the total entropy $\int_x(-\rho S)dx$. Our aim here is to construct more "faithful" approximations of the NS equations, with a discrete analogue for the precise entropy decay statement in (1.9). Our prototype result is the following.

Theorem 1.1. *Consider the NS equation* (1.1),

$$\frac{\partial}{\partial t}\mathbf{u} + \frac{\partial}{\partial x}\mathbf{f}(\mathbf{u}) = \epsilon\frac{\partial^2}{\partial x^2}\mathbf{d}(\mathbf{u}).$$

Here, $\mathbf{u} = \big[\rho, m, E\big]^\top$ *is the vector of conservative variables,* $\mathbf{f}(\mathbf{u})$ *is the corresponding 3-vector of fluxes* $\mathbf{f}(\mathbf{u}) = \big[m, qm+p, q(E+p)\big]^\top$, *and* $\epsilon\mathbf{d}(\mathbf{u})$ *stands for the combined viscous and heat fluxes,*

$$\epsilon\mathbf{d}(\mathbf{u}) = (\lambda+2\mu)\big[0, q, q^2/2\big]^\top + \kappa\big[0,0,\theta\big]^\top,$$

where ϵ signals the vanishing amplitudes of viscosity and heat conductivity. We approximate these NS equations by a semi-discrete scheme of the form

$$\begin{aligned}\frac{d}{dt}\mathbf{u}_\nu(t) &+ \frac{1}{\Delta x_\nu}\left(\mathbf{f}^*_{\nu+\frac{1}{2}} - \mathbf{f}^*_{\nu-\frac{1}{2}}\right) \\ &= \frac{\epsilon}{\Delta x_\nu}\left(\frac{\mathbf{d}(\mathbf{u}_{\nu+1}) - \mathbf{d}(\mathbf{u}_\nu)}{\Delta x_{\nu+\frac{1}{2}}} - \frac{\mathbf{d}(\mathbf{u}_\nu) - \mathbf{d}(\mathbf{u}_{\nu-1})}{\Delta x_{\nu-\frac{1}{2}}}\right). \qquad (1.10a)\end{aligned}$$

Let $\mathbf{f}^*_{\nu+\frac{1}{2}} = \mathbf{f}^*(\mathbf{u}_\nu, \mathbf{u}_{\nu+1})$ be the numerical flux given by the explicit formula,

$$\mathbf{f}^*_{\nu+\frac{1}{2}} = (\gamma - 1)\sum_{j=1}^{3}\frac{m^{j+1} - m^j}{\langle \boldsymbol{\ell}^j, \mathbf{v}_{\nu+1} - \mathbf{v}_\nu\rangle}\boldsymbol{\ell}^j, \quad \mathbf{v} = \mathbf{v}(\mathbf{u}) := \left[-\frac{E}{e} - S + \gamma + 1, \frac{q}{\theta}, -\frac{1}{\theta}\right]^\top. \qquad (1.10b)$$

Here, $\{\boldsymbol{\ell}^j = \boldsymbol{\ell}^j_{\nu+\frac{1}{2}}\}_{j=1}^3$ are three linearly independent directions in $\mathbf{v}$-space at our disposal (*consult Examples* 3.2–3.4 *below*); $\{\mathbf{r}^j = \mathbf{r}^j_{\nu+\frac{1}{2}}\}_{j=1}^3$ *is the corresponding orthogonal system and $\{m^j = m^j_{\nu+\frac{1}{2}}\}_{j=1}^4$ are the intermediate values of the momentum specified along the corresponding path, $\mathbf{v}^{j+1} = \mathbf{v}^j + \langle \boldsymbol{\ell}^j, \mathbf{v}_{\nu+1} - \mathbf{v}_\nu\rangle \mathbf{r}^j$, starting with $\mathbf{v}^1 = \mathbf{v}_\nu$ and ending with $\mathbf{v}^4 = \mathbf{v}_{\nu+1}$. Then, the resulting scheme* (1.10a), (1.10b) *is entropy stable and the following discrete entropy balance holds*[a]

$$\begin{aligned}\frac{d}{dt}\sum_\nu(-\rho_\nu S_\nu)\Delta x_\nu &= -(\lambda + 2\mu)\sum_\nu\left(\frac{\Delta q_{\nu+\frac{1}{2}}}{\Delta x_{\nu+\frac{1}{2}}}\right)^2 \widehat{(1/\theta)}_{\nu+\frac{1}{2}}\Delta x_{\nu+\frac{1}{2}} \\ &\quad - \kappa\sum_\nu\left(\frac{\Delta \theta_{\nu+\frac{1}{2}}}{\Delta x_{\nu+\frac{1}{2}}}\right)^2 \widetilde{(1/\theta)}^2_{\nu+\frac{1}{2}}\Delta x_{\nu+\frac{1}{2}} \le 0. \qquad (1.11)\end{aligned}$$

We briefly describe the content of the paper, leading to the above result. The entropy balance (1.11) is a precise discrete analogue of (1.9). The scheme (1.10a), (1.10b) contains no artificial numerical viscosity in the sense that entropy dissipation is driven solely by the viscous and heat fluxes. In the particular case that viscosity and the heat conduction are absent, $\kappa = \lambda = \mu = 0$, then the entropy balance (1.8) is reduced to the formal entropy *equality* of the Euler equations (1.5),

$$\frac{\partial}{\partial t}(-\rho S) + \frac{\partial}{\partial x}(-mS) = 0, \qquad (1.12)$$

which in turn, implies the entropy conservation $\int_x(-\rho S)(\cdot, t)\,dx = \int_x(-\rho S)(\cdot, 0)\,dx$. Similarly, setting $\epsilon\mathbf{d} = 0$, we omit the dissipative terms in NS equations, and the difference scheme (1.10a) becomes *entropy conservative*,

$$\sum(-\rho_\nu S_\nu)(t)\Delta x_\nu = \sum(-\rho_\nu S_\nu)(0)\Delta x_\nu.$$

[a]We let $\widehat{z}_{\nu+\frac{1}{2}}$ and $\widetilde{z}_{\nu+\frac{1}{2}}$ denote the arithmetic and geometric means, $\widehat{z}_{\nu+\frac{1}{2}} = (z_\nu + z_{\nu+1})/2$ and $\widetilde{z}_{\nu+\frac{1}{2}} = \sqrt{z_\nu z_{\nu+1}}$.

Entropy conservative schemes are studied in Sec. 3, following [24]. The key ingredient here is the construction of their entropy conservative fluxes, such as $\mathbf{f}^*_{\nu+\frac{1}{2}}$ in (1.10b). These fluxes employ the so called entropy variables, $\mathbf{v} = \mathbf{v}(\mathbf{u})$, which are discussed in Sec. 2. The main results are then summarized in Theorems 3.1 and 3.6. Finally, in Sec. 4, we present a series of numerical simulations with the new schemes. The entropy conservative approximations of Euler equations are "purely dispersive" and as such, their solutions experience dispersive oscillations, interesting for their own sake, consult [6–9, 11, 12, 14, 15, 22] and the references therein. Turning to the NS equations, our simulations provide a remarkable evidence for the different roles that viscosity and heat conduction have in removing the dispersive oscillations, to yield sharp monotone profiles of well-resolved shock and contact layers. No limiters were added, but instead, the viscous and heat conduction terms in NS equations are found to serve as accurate edge detectors.

Remark 1.2. The viscous NS equations dissipate a general family of entropies, $-\rho h(S)$, where $h(S)$ is an arbitrary increasing function. Indeed, arguing along the above lines we multiply the continuity equation by $h(S)$ and adding it to (1.7) $\times\, h'(S)$ to find

$$\frac{\partial}{\partial t}\big(-\rho h(S)\big) + \frac{\partial}{\partial x}\big(-mh(S) + \kappa(\ln\theta)_x h'(S)\big) = \kappa h''(S) S_x \frac{\theta_x}{\theta} - h'(S)\left((\lambda+2\mu)\frac{q_x^2}{\theta} + \kappa\left(\frac{\theta_x}{\theta}\right)^2\right). \tag{1.13}$$

In the case that the heat conduction is absent, the first term on the right-hand side of (1.13) vanishes, and we are left with

$$\frac{d}{dt}\int_x \big(-\rho h(S)\big)dx = -(\lambda+2\mu)\int_x \frac{q_x^2}{\theta} h'(S)dx. \tag{1.14}$$

Thus, the viscous NS equations imply the dissipation of a family of entropies, $\int_x(-\rho h(S))\,dx$ for all $h'(S) > 0$; consult [5]. Each one of these entropies carries its own entropy conservative flux $\mathbf{f}^*_{\nu+\frac{1}{2}}$. The explicit construction of such fluxes is outlined in Theorem 3.1 below. Combining these entropy conservative fluxes together with centered differencing of the additional viscous terms, $(\lambda+2\mu)[0, q, q^2/2]^\top$, yield a generalization of Theorem 1.1 which recovers the precise entropy balance (1.14).

We note in passing that when heat conduction is present, however, the negativity of the first term on the right of (1.13) requires $h''(S) = 0$, so that we are left with one canonical entropy, $h(S) \sim S$ discussed in Theorem 1.1; consult [6–9].

Remark 1.3. It is straightforward to generalize the recipe for "faithful" entropy stable approximations of *multidimensional* NS equations. The extension is carried out dimension by dimension and as indicated in the one-dimensional setup of Theorem 1.1, one has the freedom of choosing different paths in phase space.

2. Entropy Dissipation

2.1. *The entropy variables*

We turn our attention to general systems of hyperbolic conservation laws

$$\frac{\partial}{\partial t}\mathbf{u} + \frac{\partial}{\partial x}\mathbf{f}(\mathbf{u}) = 0, \quad (x,t) \in \mathbb{R} \times [0,\infty), \tag{2.1}$$

governing the N-vector of conserved variables, $\mathbf{u} = [u_1, \ldots, u_N]^\top$. The entropy equality

$$\frac{\partial}{\partial t}U(\mathbf{u}) + \frac{\partial}{\partial x}F(\mathbf{u}) = 0 \tag{2.2}$$

is an additional conservation law for an entropy function, $U(\mathbf{u})$, which is balanced by an entropy flux $F(\mathbf{u})$. The Euler equations (1.5) are viewed as a prototype example for such systems, with the three conservative variables $\mathbf{u} = \big[\rho, m, E\big]^\top$ balanced by the flux $\mathbf{f} = \big[m, qm + p, q(E+p)\big]^\top$ and endowed with entropy pairs $(U,F) = \big(-\rho h(S),\, -mh(S)\big)$. We now briefly recall the circle of ideas linking the dissipation of the total entropy, $\int_x U(\mathbf{u}(\cdot,t))dx$, and the realization of $\mathbf{u}$ as a vanishing viscosity limit, in analogy to the vanishing NS limits and their relation to entropic solutions of the Euler equations. We refer to e.g. [1,16], for a more comprehensive discussion.

Let $(U(\mathbf{u}), F(\mathbf{u}))$ be a given entropy pair associated with (2.1). Note that $U(\mathbf{u})$ satisfies the entropy equality (2.2) if and only if it is linked to an entropy flux function $F(\mathbf{u})$ through the compatibility relation

$$U_{\mathbf{u}}^\top \mathbf{f}_{\mathbf{u}} = F_{\mathbf{u}}^\top. \tag{2.3}$$

Indeed, multiplying (2.1) by $U_{\mathbf{u}}^\top$ on the left, one recovers the equivalence between (2.2) and (2.3) for all $\mathbf{u}$'s solving (2.1). Of course, these formal manipulations are valid only under the smooth regime. To justify these steps in the presence of shock discontinuities, the conservation law (2.1) is realized by appropriate vanishing viscosity limits. To this end, we define the *entropy variables* $\mathbf{v}(\mathbf{u}) := U_{\mathbf{u}}(\mathbf{u})$. We make the additional assumption that the entropy $U(\mathbf{u})$ is *convex*, so that the mapping $\mathbf{u} \mapsto \mathbf{v}$ is a one-to-one. Following [2, 17], we claim that the change of variables, $\mathbf{u} = \mathbf{u}(\mathbf{v})$, puts the system (2.1) into the equivalent *symmetric* form,

$$\frac{\partial}{\partial t}\mathbf{u}(\mathbf{v}) + \frac{\partial}{\partial x}\mathbf{f}(\mathbf{u}(\mathbf{v})) = 0. \tag{2.4}$$

The system (2.4) is symmetric in the sense that the Jacobian matrices of fluxes are,[b]

$$\mathbf{u}_{\mathbf{v}}(\mathbf{v}) = \big(\mathbf{u}_{\mathbf{v}}(\mathbf{v})\big)^\top \quad \text{and} \quad \mathbf{f}_{\mathbf{v}}(\mathbf{v}) = \big(\mathbf{f}_{\mathbf{v}}(\mathbf{v})\big)^\top. \tag{2.5}$$

[b]For brevity of notations we often write $\mathbf{f}(\mathbf{v})$ for $\mathbf{f}(\mathbf{u}(\mathbf{v}))$ whenever the different dependence of $\mathbf{f}(\mathbf{u})$ and $\mathbf{f}(\mathbf{v})$ is made clear by the distinction between the conservative variables $\mathbf{u}$ and entropy variables $\mathbf{v}$.

Indeed, a straightforward computation utilizing the compatibility relation (2.3), shows that $\mathbf{u}(\mathbf{v})$ and $\mathbf{f}(\mathbf{v})$ are, respectively, the gradients of the corresponding potential functions, ϕ and ψ,

$$\mathbf{u}(\mathbf{v}) = \phi_{\mathbf{v}}(\mathbf{v}), \quad \phi(\mathbf{v}) := \langle \mathbf{v}, \mathbf{u}(\mathbf{v})\rangle - U(\mathbf{u}(\mathbf{v})), \tag{2.6}$$

$$\mathbf{f}(\mathbf{v}) = \psi_{\mathbf{v}}(\mathbf{v}), \quad \psi(\mathbf{v}) := \langle \mathbf{v}, \mathbf{f}(\mathbf{v})\rangle - F(\mathbf{u}(\mathbf{v})). \tag{2.7}$$

Hence the Jacobian matrices $H(\mathbf{v}) := \mathbf{u}_{\mathbf{v}}(\mathbf{v})$ and $B(\mathbf{v}) := \mathbf{f}_{\mathbf{v}}(\mathbf{v})$ in (2.5) are symmetric, being Hessians of the potentials $\phi(\mathbf{v})$ and $\psi(\mathbf{v})$. Moreover, the convexity of $U(\cdot)$ implies that H is positive definite, $H = (U_{\mathbf{uu}})^{-1} > 0$.

Physically relevant solutions of (2.1) are postulated as limits of the vanishing viscosity solutions,

$$\frac{\partial}{\partial t}\mathbf{u}^{\epsilon} + \frac{\partial}{\partial x}\mathbf{f}(\mathbf{u}^{\epsilon}) = \epsilon\frac{\partial^2}{\partial x^2}\mathbf{d}(\mathbf{u}^{\epsilon}), \tag{2.8}$$

where $\mathbf{d}(\mathbf{u})$ is any *admissible* dissipative flux, and $\epsilon \downarrow 0$ stands for vanishing amplitudes such as the viscosity coefficients λ, μ, the heat conductivity κ, etc. Here, the admissibility of the dissipative flux requires the Jacobian $\mathbf{d}_{\mathbf{u}}$ to be H-symmetric positive-definite, that is,

$$\mathbf{d}_H = (\mathbf{d}_H)^{\top} \geq 0, \quad \mathbf{d}_H := \mathbf{d}_{\mathbf{u}}H. \tag{2.9}$$

If we express the dissipation flux in terms of the entropy variables, $\mathbf{d}(\mathbf{v}) = \mathbf{d}(\mathbf{u}(\mathbf{v}))$, then admissibility requires that the $\mathbf{v}$-Jacobian of this flux will be positive symmetric, $\mathbf{d}_H = \mathbf{d}_{\mathbf{v}}(\mathbf{v}) = \mathbf{d}_{\mathbf{v}}^{\top}(\mathbf{v}) \geq 0$. Thus, in this case (2.8) reads

$$\frac{\partial}{\partial t}\mathbf{u}(\mathbf{v}^{\epsilon}) + \frac{\partial}{\partial x}\mathbf{f}(\mathbf{v}^{\epsilon}) = \epsilon\frac{\partial^2}{\partial x^2}\mathbf{d}(\mathbf{v}^{\epsilon}),$$

and all $\mathbf{v}$-dependent fluxes — the temporal, spatial and the dissipation flux have symmetric Jacobains.

We now integrate (2.8) against $\mathbf{v}^{\top} = U_{\mathbf{u}}^{\top}$, employ the compatibility relation $U_{\mathbf{u}}^{\top}\mathbf{f}_x = F_x^{\top}$ and use "differentiation by parts" on the admissible dissipation on the right to find

$$\frac{\partial}{\partial t}U(\mathbf{u}^{\epsilon}) + \frac{\partial}{\partial x}\big(F^{\epsilon}(\mathbf{u}^{\epsilon}) - \epsilon\big\langle \mathbf{v}^{\epsilon}, \mathbf{d}(\mathbf{u}^{\epsilon})_x\big\rangle\big) = -\epsilon\big\langle \mathbf{v}_x^{\epsilon}, \mathbf{d}_{\mathbf{v}}\mathbf{v}_x^{\epsilon}\big\rangle \leq 0. \tag{2.10}$$

Letting $\epsilon \downarrow 0$, we obtain the *entropy inequality*, see [10]

$$\frac{\partial}{\partial t}U(\mathbf{u}) + \frac{\partial}{\partial x}F(\mathbf{u}) \leq 0, \tag{2.11}$$

which is the generalization of the entropy decay statements for NS equations (1.8) and (1.13).

2.2. *Examples of entropy pairs for Navier–Stokes equations*

The NS equations admit the family of convex entropy pairs

$$U(\mathbf{u}) = -\rho h(S), \quad F(\mathbf{u}) = -mh(S), \quad h'(\cdot) \geq 0. \tag{2.12}$$

Here $S = \ln(p\rho^{-\gamma})$ is the specific entropy and the convexity of the corresponding $U(\mathbf{u})$'s as functions of $\mathbf{u} = (\rho, m, E)^\top$ holds if and only if $h'(S) - \gamma h''(S) > 0$, see [5]. We consider two prototype examples.

Example 2.1. The simplest choice of $h(S)$ is the specific entropy S itself,

$$h(S) = S = \ln\bigl(p\rho^{-\gamma}\bigr)\,. \tag{2.13}$$

Straightforward computation gives us the following entropy pair, entropy variables, and potentials.

- Entropy pair $U(\mathbf{u}) = -\rho S$ and $F(\mathbf{u}) = -mS$.
- Entropy variable (consult [5])

$$\mathbf{v}(\mathbf{u}) = \begin{bmatrix} -E/e - S + \gamma + 1 \\ q/\theta \\ -1/\theta \end{bmatrix} \tag{2.14}$$

  with the inverse mapping

$$\mathbf{u}(\mathbf{v}) = \frac{p}{\gamma - 1}\begin{bmatrix} -v_3 \\ v_2 \\ 1 - \frac{v_2^2}{2v_3} \end{bmatrix} = w \begin{bmatrix} -v_3 \\ v_2 \\ 1 - \frac{v_2^2}{2v_3} \end{bmatrix},$$

  where $w = \left(\frac{\gamma-1}{(-v_3)^\gamma}\right)^{\frac{1}{\gamma-1}} e^{\left(\frac{-S}{\gamma-1}\right)}$, $S = \gamma - v_1 + \frac{v_2^2}{2v_3}$.
- Potential pair $\phi = (\gamma - 1)\rho$ and $\psi = (\gamma - 1)m$.

In this case, the general statement of entropy balance in (2.10) with the entropy pair $(U, F) = (-\rho S, -mS)$ amounts to the one we have in (1.9),

$$\frac{d}{dt}\int_x -(\rho S)dx = -\epsilon \int_x \langle \mathbf{v}_x^\epsilon, \mathbf{d}_\mathbf{v}\mathbf{v}_x^\epsilon\rangle\, dx = -(\lambda + 2\mu)\int_x \frac{q_x^2}{\theta} dx - \kappa \int_x \frac{\theta_x^2}{\theta^2} dx \leq 0. \tag{2.15}$$

Example 2.2. A particularly convenient form of entropy variables is associated the entropy function (consult [5, 24]),

$$U(\mathbf{u}) = -\rho h(S) \quad \text{with } h(S) = \frac{\gamma + 1}{\gamma - 1} e^{\frac{S}{\gamma+1}}, \tag{2.16}$$

where we have the following.

- Entropy pair $U(\mathbf{u}) = \dfrac{1+\gamma}{1-\gamma}(\rho p)^{\frac{1}{1+\gamma}}$ and $F(\mathbf{u}) = \dfrac{1+\gamma}{1-\gamma} q(\rho p)^{\frac{1}{1+\gamma}}$.

- Entropy variable $\mathbf{v}(\mathbf{u}) = \nabla_{\mathbf{u}} U(\mathbf{u}) = -(\rho p)^{-\frac{\gamma}{1+\gamma}} \begin{bmatrix} E \\ -m \\ \rho \end{bmatrix}$
  with the inverse mapping

$$\mathbf{u}(\mathbf{v}) = -(\rho p)^{\frac{\gamma}{\gamma+1}} \begin{bmatrix} v_3 \\ -v_2 \\ v_1 \end{bmatrix} = -\left[(\gamma-1)\left(v_1 v_3 - \frac{v_2^2}{2}\right)\right]^{\frac{\gamma}{1-\gamma}} \begin{bmatrix} v_3 \\ -v_2 \\ v_1 \end{bmatrix}.$$

- Potential pair $(\phi, \psi) = \big((\rho p)^{\frac{1}{\gamma+1}}, m(p\rho^{-\gamma})^{\frac{1}{\gamma+1}}\big)$.

In case that the heat conduction is absent ($\kappa = 0$), we apply the general statement of entropy balance (2.10) with the entropy pair, $(U,\, F) = \frac{1+\gamma}{1-\gamma}\big((\rho p)^{\frac{1}{1+\gamma}}, q(\rho p)^{\frac{1}{1+\gamma}}\big)$, obtaining

$$\begin{aligned} \frac{d}{dt}\int_x -(\rho p)^{\frac{1}{1+\gamma}} dx &= -\epsilon \int_x \langle \mathbf{v}_x^\epsilon,\, \mathbf{d}_{\mathbf{v}} \mathbf{v}_x^\epsilon \rangle dx \\ &\equiv -(\lambda + 2\mu) \int_x \frac{(\gamma-1)h'(S)q_x^2}{(1+\gamma)\theta} dx \\ &= -\frac{\lambda+2\mu}{1+\gamma} \int_x \frac{e^{S/(1+\gamma)} q_x^2}{\theta} dx \le 0. \end{aligned} \tag{2.17}$$

Remark 2.3. As noted in [5], the flux $\mathbf{f}(\mathbf{v})$ is a homogeneous function of degree $\eta =: (1+\gamma)/(1-\gamma)$, $\mathbf{f}(\alpha \mathbf{v}) = \alpha^\eta \mathbf{f}(\mathbf{v})$, $\quad \forall\, \alpha \in \mathbb{R}$. Homogeneity implies that $\mathbf{f}_{\mathbf{v}}(\mathbf{v})\mathbf{v} = \eta \mathbf{f}(\mathbf{v})$ which in turn, enables us to rewrite the spatial flux in (2.1) in a skew-adjoint form, $\mathbf{f}(\mathbf{u})_x = \big(\mathbf{f}_{\mathbf{v}} \mathbf{v}_x + (\mathbf{f}_{\mathbf{v}} \mathbf{v})_x\big)/(\eta+1)$; consult [20].

3. Entropy Stable Schemes for Navier–Stokes Equations

3.1. *Entropy conservative schemes*

We turn our attention to consistent approximations of (2.1), based on semi-discrete conservative schemes of the form

$$\frac{d}{dt}\mathbf{u}_\nu(t) = -\frac{1}{\Delta x_\nu}\big(\mathbf{f}_{\nu+\frac{1}{2}} - \mathbf{f}_{\nu-\frac{1}{2}}\big). \tag{3.1}$$

Here, $\mathbf{u}_\nu(t)$ denotes the discrete solution along the grid line (x_ν, t), $\Delta x_\nu := \frac{1}{2}(x_{\nu+1} - x_{\nu-1})$ is the possibly variable mesh spacing and $\mathbf{f}_{\nu+\frac{1}{2}}$ is the Lipschitz-continuous numerical flux which occupies a stencil of $(2p+1)$-gridvalues,

$$\mathbf{f}_{\nu+\frac{1}{2}} = \mathbf{f}(\mathbf{u}_{\nu-p+1}, \ldots, \mathbf{u}_{\nu+p}).$$

The scheme is said to be consistent with the system (2.1) if $\mathbf{f}$ satisfies $\mathbf{f}(\mathbf{u}, \mathbf{u}, \ldots, \mathbf{u}) = \mathbf{f}(\mathbf{u})$, $\forall \mathbf{u} \in \mathbb{R}^N$. By making the changes of variables $\mathbf{u}_\nu = \mathbf{u}(\mathbf{v}_\nu)$, we obtain the equivalent form of (3.1)

$$\frac{d}{dt}\mathbf{u}(\mathbf{v}_\nu(t)) = -\frac{1}{\Delta x_\nu}\big(\mathbf{f}_{\nu+\frac{1}{2}} - \mathbf{f}_{\nu-\frac{1}{2}}\big). \tag{3.2}$$

The essential difference lies with the numerical flux, $\mathbf{f}_{\nu+\frac{1}{2}}$, which is now expressed in terms of the entropy variables,

$$\mathbf{f}_{\nu+\frac{1}{2}} = \mathbf{f}(\mathbf{v}_{\nu-p+1},\ldots,\mathbf{v}_{\nu+p}) := \mathbf{f}(\mathbf{u}\left(\mathbf{v}_{\nu-p+1}\right),\ldots,\mathbf{u}\left(\mathbf{v}_{\nu+p}\right)),$$

consistent with the differential flux,

$$\mathbf{f}(\mathbf{v},\mathbf{v},\ldots,\mathbf{v}) = \mathbf{f}(\mathbf{v}) \equiv \mathbf{f}(\mathbf{u}(\mathbf{v})). \tag{3.3}$$

The semi-discrete schemes (3.1) and (3.2) are completely identical. It proved useful, however, to work with the entropy variables rather than the usual conservative ones, since system (2.1) is symmetrized with respect to these entropy variables. The entropy variables-based formula (3.2) has the advantage that it provides a natural ordering of symmetric matrices, which in turn enables us to *compare* the numerical viscosities of different schemes, consult [21, 23] for details. In particular, we will be able to utilize the entropy conservative discretization of [24] for the Euler convective part of the equations, and thus recover the precise entropy balance dictated by viscous and heat fluxes in NS equations.

Let (U, F) be a given entropy pair. We proceed with the construction of an *entropy conservative* scheme, in the sense of satisfying a discrete *entropy equality* analogous to (2.2),

$$\frac{d}{dt}U(\mathbf{u}_\nu(t)) + \frac{1}{\Delta x_\nu}\big(F_{\nu+\frac{1}{2}} - F_{\nu-\frac{1}{2}}\big) = 0. \tag{3.4}$$

Here, $F_{\nu+\frac{1}{2}} = F(\mathbf{u}_{\nu-p+1},\ldots,\mathbf{u}_{\nu+p})$ is a consistent numerical entropy flux, such that $F(\mathbf{u},\mathbf{u},\ldots,\mathbf{u}) = F(\mathbf{u})$, $\forall \mathbf{u} \in \mathbb{R}^N$. The numerical flux of such entropy conservative schemes will play an essential role in the construction of entropy stable schemes, by adding a judicious amount of physical viscosity.

The key step in the construction of entropy conservative schemes is the choice of *an arbitrary* piecewise-constant path in phase space, connecting two neighboring gridvalues $\mathbf{v}_\nu$ and $\mathbf{v}_{\nu+1}$ through the intermediate states $\{\mathbf{v}^j_{\nu+\frac{1}{2}}\}_{j=1}^N$ at the spatial cell $[x_\nu, x_{\nu+1}]$. Let $\{\mathbf{r}^j_{\nu+\frac{1}{2}}\}_{j=1}^N$ be an arbitrary set of N linearly independent N-vectors, and let $\{\boldsymbol{\ell}^j_{\nu+\frac{1}{2}}\}_{j=1}^N$ be the corresponding orthogonal set. We introduce the intermediate gridvalues $\{\mathbf{v}^j_{\nu+\frac{1}{2}}\}_{j=2}^N$, which define a piecewise constant path in phase space

$$\begin{cases} \mathbf{v}^1_{\nu+\frac{1}{2}} = \mathbf{v}_\nu, \\ \mathbf{v}^{j+1}_{\nu+\frac{1}{2}} = \mathbf{v}^j_{\nu+\frac{1}{2}} + \big\langle \boldsymbol{\ell}^j_{\nu+\frac{1}{2}}, \Delta\mathbf{v}_{\nu+\frac{1}{2}}\big\rangle \mathbf{r}^j_{\nu+\frac{1}{2}}, \\ \qquad\qquad j = 1,2,\ldots,N-1, \;\; \Delta\mathbf{v}_{\nu+\frac{1}{2}} := \mathbf{v}_{\nu+1} - \mathbf{v}_\nu, \\ \mathbf{v}^{N+1}_{\nu+\frac{1}{2}} = \mathbf{v}_{\nu+1}. \end{cases} \tag{3.5}$$

Theorem 3.1 [24, Theorem 6.1]. *Consider the system of conservation laws* (2.1). *Given the entropy pair* (U, F), *then the conservative scheme*

$$\frac{d}{dt}\mathbf{u}_\nu(t) = -\frac{1}{\Delta x_\nu}\left(\mathbf{f}^*_{\nu+\frac{1}{2}} - \mathbf{f}^*_{\nu-\frac{1}{2}}\right) \tag{3.6}$$

with a 2-point numerical flux $\mathbf{f}^*_{\nu+\frac{1}{2}} = \mathbf{f}(\mathbf{v}_\nu, \mathbf{v}_{\nu+1})$,

$$\mathbf{f}^*_{\nu+\frac{1}{2}} = \sum_{j=1}^{N} \frac{\psi\left(\mathbf{v}^{j+1}_{\nu+\frac{1}{2}}\right) - \psi\left(\mathbf{v}^{j}_{\nu+\frac{1}{2}}\right)}{\left\langle \boldsymbol{\ell}^j_{\nu+\frac{1}{2}}, \Delta\mathbf{v}_{\nu+\frac{1}{2}}\right\rangle} \boldsymbol{\ell}^j_{\nu+\frac{1}{2}} \tag{3.7}$$

is an entropy-conservative approximation, consistent with (2.1), (2.2). *Here,* $\mathbf{v}$ *are the entropy variables,* $\mathbf{v} = U_{\mathbf{u}}(\mathbf{u})$ *and* $\psi(\mathbf{v})$ *is the entropy potential* (2.7) $\psi(\mathbf{v}) = \langle \mathbf{v}, \mathbf{f}(\mathbf{u}(\mathbf{v}))\rangle - F(\mathbf{u}(\mathbf{v}))$.

Proof. The proof is based on the requirement of entropy conservation in [23, Theorem 5.2],

$$\left\langle \Delta\mathbf{v}_{\nu+\frac{1}{2}}, \mathbf{f}^*_{\nu+\frac{1}{2}}\right\rangle = \Delta\psi_{\nu+\frac{1}{2}}, \quad \Delta\psi_{\nu+\frac{1}{2}} := \psi(\mathbf{v}_{\nu+1}) - \psi(\mathbf{v}_\nu). \tag{3.8}$$

The numerical flux (3.7) satisfies this entropy conservation requirement, for

$$\begin{aligned}\left\langle \Delta\mathbf{v}_{\nu+\frac{1}{2}}, \mathbf{f}^*_{\nu+\frac{1}{2}}\right\rangle &= \sum_{j=1}^{N} \frac{\psi\left(\mathbf{v}^{j+1}_{\nu+\frac{1}{2}}\right) - \psi\left(\mathbf{v}^{j}_{\nu+\frac{1}{2}}\right)}{\left\langle \boldsymbol{\ell}^j_{\nu+\frac{1}{2}}, \Delta\mathbf{v}_{\nu+\frac{1}{2}}\right\rangle} \left\langle \boldsymbol{\ell}^j_{\nu+\frac{1}{2}}, \Delta\mathbf{v}_{\nu+\frac{1}{2}}\right\rangle \\ &= \sum_{j=1}^{N} \psi\left(\mathbf{v}^{j+1}_{\nu+\frac{1}{2}}\right) - \psi\left(\mathbf{v}^{j}_{\nu+\frac{1}{2}}\right) = \psi\left(\mathbf{v}^{N+1}_{\nu+\frac{1}{2}}\right) - \psi\left(\mathbf{v}^{1}_{\nu+\frac{1}{2}}\right) = \Delta\psi_{\nu+\frac{1}{2}}.\end{aligned}$$

In addition, $\mathbf{f}^*_{\nu+\frac{1}{2}}$ is a consistent flux satisfying (3.3). Indeed, if we let $\mathbf{v}^{j+\frac{1}{2}}_{\nu+\frac{1}{2}}(\xi)$ denote intermediate path, $\mathbf{v}^{j+\frac{1}{2}}_{\nu+\frac{1}{2}}(\xi) := \left(\mathbf{v}^j_{\nu+\frac{1}{2}} + \mathbf{v}^{j+1}_{\nu+\frac{1}{2}}\right)/2 + \xi\left\langle \boldsymbol{\ell}^j_{\nu+\frac{1}{2}}, \Delta\mathbf{v}_{\nu+\frac{1}{2}}\right\rangle \mathbf{r}^j_{\nu+\frac{1}{2}}$ connecting $\mathbf{v}^j_{\nu+\frac{1}{2}}$ and $\mathbf{v}^{j+1}_{\nu+\frac{1}{2}}$, then by (2.7), we have

$$\begin{aligned}\psi\left(\mathbf{v}^{j+1}_{\nu+\frac{1}{2}}\right) - \psi\left(\mathbf{v}^{j}_{\nu+\frac{1}{2}}\right) &= \int_{\xi=-\frac{1}{2}}^{\frac{1}{2}} \frac{d}{d\xi}\psi\left(\mathbf{v}^{j+\frac{1}{2}}_{\nu+\frac{1}{2}}(\xi)\right) d\xi \\ &= \left\langle \int_{\xi=-\frac{1}{2}}^{\frac{1}{2}} \mathbf{f}\left(\mathbf{v}^{j+\frac{1}{2}}_{\nu+\frac{1}{2}}(\xi)\right) d\xi, \mathbf{r}^j_{\nu+\frac{1}{2}}\right\rangle \left\langle \boldsymbol{\ell}^j_{\nu+\frac{1}{2}}, \Delta\mathbf{v}_{\nu+\frac{1}{2}}\right\rangle.\end{aligned}$$

Inserted into (3.7), we can rewrite the entropy-conservative flux (3.7) in the equivalent form

$$\mathbf{f}^*_{\nu+\frac{1}{2}} = \sum_{j=1}^{N} \left\langle \int_{\xi=-\frac{1}{2}}^{\frac{1}{2}} \mathbf{f}\left(\mathbf{v}^{j+\frac{1}{2}}_{\nu+\frac{1}{2}}(\xi)\right) d\xi, \mathbf{r}^j_{\nu+\frac{1}{2}}\right\rangle \boldsymbol{\ell}^j_{\nu+\frac{1}{2}}, \tag{3.9}$$

and the consistency relation (3.3) now follows, $\mathbf{f}^*(\mathbf{v}, \mathbf{v}) = \sum_{j=1}^{N} \left\langle \mathbf{f}(\mathbf{v}), \mathbf{r}^j_{\nu+\frac{1}{2}}\right\rangle \boldsymbol{\ell}^j_{\nu+\frac{1}{2}} = \mathbf{f}(\mathbf{v})$. □

We emphasize that the recipe for construction entropy-conservative fluxes in (3.7) allows an *arbitrary* choice of a path in phase space. We demonstrate this recipe with three examples.

Example 3.2. Set $\{\mathbf{r}^j\}$ along the standard Cartesian coordinates, $\mathbf{r}^j_{\nu+\frac{1}{2}} = \mathbf{e}_j$, $j = 1, 2, \ldots, N$. In this case we have

$$\mathbf{v}^j_{\nu+\frac{1}{2}} = \left[(\mathbf{v}_{\nu+1})_1, \ldots, (\mathbf{v}_{\nu+1})_{j-1}, (\mathbf{v}_\nu)_j, \ldots, (\mathbf{v}_\nu)_N\right]^\top, \quad j = 2, 3, \ldots, N-1,$$

and the entropy conservative flux (3.7) is given by the particularly simple explicit formula

$$\mathbf{f}^*_{\nu+\frac{1}{2}} = \left[\frac{\psi(\mathbf{v}^2_{\nu+\frac{1}{2}}) - \psi(\mathbf{v}_\nu)}{(\mathbf{v}_{\nu+1})_1 - (\mathbf{v}_\nu)_1}, \ldots, \frac{\psi(\mathbf{v}^{j+1}_{\nu+\frac{1}{2}}) - \psi(\mathbf{v}^j_{\nu+\frac{1}{2}})}{(\mathbf{v}_{\nu+1})_j - (\mathbf{v}_\nu)_j}, \ldots, \frac{\psi(\mathbf{v}_{\nu+1}) - \psi(\mathbf{v}^N_{\nu+\frac{1}{2}})}{(\mathbf{v}_{\nu+1})_N - (\mathbf{v}_\nu)_N}\right]^\top. \tag{3.10}$$

We carried out numerical experiments with these fluxes for the approximate solution of Euler and NS equations. The formulation is particularly simple though the computed intermediate values might lie outside the physical space ρ, $p > 0$.

Example 3.3. A more "physically relevant" choice than the Cartesian path is offered by a Riemann path which consists of $\{\mathbf{u}^j_{\nu+\frac{1}{2}}\}_{j=1}^N$, stationed along an (approximate) set of right eigenvectors, $\{\widehat{\mathbf{r}}^j_{\nu+\frac{1}{2}}\}$, of the Jacobian $\mathbf{f}_\mathbf{u}(\mathbf{u}_{\nu+\frac{1}{2}})$. Set $\mathbf{v}^j_{\nu+\frac{1}{2}} = \mathbf{v}(\mathbf{u}^j_{\nu+\frac{1}{2}})$, $j = 1, 2, \ldots, N$, and let $\boldsymbol{\ell}^j$'s be the orthogonal system to $\{\mathbf{v}^{j+1} - \mathbf{v}^j\}_{j=1}^N$. This will be our choice of a path for computing entropy stable approximations of NS equations in Sec. 3.2 below. The resulting flux, mixing conservative and entropy variables, admits the somewhat simpler form

$$\mathbf{f}^*_{\nu+\frac{1}{2}} = \sum_{j=1}^N \frac{\psi(\mathbf{u}^{j+1}_{\nu+\frac{1}{2}}) - \psi(\mathbf{u}^j_{\nu+\frac{1}{2}})}{\langle \boldsymbol{\ell}^j_{\nu+\frac{1}{2}}, \Delta\mathbf{v}_{\nu+\frac{1}{2}}\rangle} \boldsymbol{\ell}^j_{\nu+\frac{1}{2}} \quad \text{where } \psi(\mathbf{u}) = \langle U_\mathbf{u}(\mathbf{u}), \mathbf{f}(\mathbf{u})\rangle - F(\mathbf{u}). \tag{3.11}$$

Example 3.4. If all $\mathbf{r}^j$'s are chosen to approach the same direction of $\Delta\mathbf{v}_{\nu+\frac{1}{2}}$, then by (3.9), the flux (3.9) "collapses" to the entropy-conservative flux

$$\mathbf{f}^*_{\nu+\frac{1}{2}} = \int_{\xi=-\frac{1}{2}}^{\frac{1}{2}} \mathbf{f}(\mathbf{v}_{\nu+\frac{1}{2}}(\xi))d\xi, \quad \mathbf{v}_{\nu+\frac{1}{2}}(\xi) := \frac{1}{2}(\mathbf{v}_\nu + \mathbf{v}_{\nu+1}) + \xi\Delta\mathbf{v}_{\nu+\frac{1}{2}}. \tag{3.12}$$

The resulting flux (3.12) was introduced in [22] and was the forerunner for the family of entropy conservative fluxes outlined in Theorem 3.1. It has the drawback, however, that its evaluation requires a nonlinear integration in phase space. Thus, with the loss of linear independence, we lose here the *explicit* evaluation of the entropy conservative flux offered in (3.7) and demonstrated in the previous two examples.

3.2. *Entropy stable semi-discrete schemes for Navier–Stokes equations*

3.2.1. *The compressible Euler equations*

Let (U, F) be an admissible entropy pair associated with the Euler equations (1.5), let $\mathbf{v} = \mathbf{v}(\mathbf{u})$ denote the corresponding entropy variables outlined in Examples 2.1 and 2.2 above. To conserve the total entropy $\int_x U(\mathbf{u}(\cdot, t))dx$, we appeal to the semi-discrete scheme (3.6) with the entropy-conservative numerical flux (3.7),

$$\mathbf{f}^*_{\nu+\frac{1}{2}} = \sum_{j=1}^{3} \frac{\psi\big(\mathbf{v}^{j+1}_{\nu+\frac{1}{2}}\big) - \psi\big(\mathbf{v}^{j}_{\nu+\frac{1}{2}}\big)}{\big\langle \boldsymbol{\ell}^j_{\nu+\frac{1}{2}}, \Delta\mathbf{v}_{\nu+\frac{1}{2}}\big\rangle} \boldsymbol{\ell}^j_{\nu+\frac{1}{2}}.$$

To compute $\mathbf{f}^*_{\nu+\frac{1}{2}}$, we distinguish between two cases. If $\mathbf{v}_\nu = \mathbf{v}_{\nu+1}$, we employ the equivalent form of the numerical flux in (3.9),

$$\mathbf{f}^*_{\nu+\frac{1}{2}} = \sum_{j=1}^{3} \left\langle \int_{\xi=-\frac{1}{2}}^{\frac{1}{2}} \mathbf{f}\left(\mathbf{v}^{j+\frac{1}{2}}_{\nu+\frac{1}{2}}(\xi)\right) d\xi, \mathbf{r}^j_{\nu+\frac{1}{2}} \right\rangle \boldsymbol{\ell}^j_{\nu+\frac{1}{2}},$$

which implies that all the intermediate gridvalues coincide, $\mathbf{v}_\nu = \mathbf{v}^1_{\nu+\frac{1}{2}} = \mathbf{v}^2_{\nu+\frac{1}{2}} = \mathbf{v}^3_{\nu+\frac{1}{2}} = \mathbf{v}^4_{\nu+\frac{1}{2}} = \mathbf{v}_{\nu+1}$ and the entropy-conservative flux amounts to $\mathbf{f}^*_{\nu+\frac{1}{2}} = \mathbf{f}_\nu = \mathbf{f}_{\nu+1}$. Otherwise, if $\mathbf{v}_\nu \neq \mathbf{v}_{\nu+1}$, we choose to work along the path which is dictated by an (approximate) Riemann solver. Specifically, we use the eigensystem of the Roe matrix, $[A]_{\nu+\frac{1}{2}} = A(\mathbf{u}_\nu, \mathbf{u}_{\nu+1})$, see [18],

$$[A]_{\nu+\frac{1}{2}} := \begin{bmatrix} 0 & 1 & 0 \\ \frac{\gamma-3}{2}\bar{q}^2_{\nu+\frac{1}{2}} & (3-\gamma)\bar{q}_{\nu+\frac{1}{2}} & \gamma-1 \\ \frac{\gamma-1}{2}\bar{q}^3_{\nu+\frac{1}{2}} - \bar{q}_{\nu+\frac{1}{2}}\bar{H}_{\nu+\frac{1}{2}} & \bar{H}_{\nu+\frac{1}{2}} - (\gamma-1)\bar{q}^2_{\nu+\frac{1}{2}} & \gamma\bar{q}_{\nu+\frac{1}{2}} \end{bmatrix}. \tag{3.13a}$$

Here $\bar{q}$ and $\bar{H}$ are the average values of the velocity q and total enthalpy $H = (E+p)/\rho$ at Roe-average state,

$$\bar{q}_{\nu+\frac{1}{2}} = \frac{q_\nu\sqrt{\rho_\nu} + q_{\nu+1}\sqrt{\rho_{\nu+1}}}{\sqrt{\rho_\nu} + \sqrt{\rho_{\nu+1}}}, \quad \bar{H}_{\nu+\frac{1}{2}} = \frac{H_\nu\sqrt{\rho_\nu} + H_{\nu+1}\sqrt{\rho_{\nu+1}}}{\sqrt{\rho_\nu} + \sqrt{\rho_{\nu+1}}}. \tag{3.13b}$$

The $\widehat{\mathbf{r}}^j$'s are the right eigenvectors $\{\widehat{\mathbf{r}}^j \equiv \widehat{\mathbf{r}}^j_{\nu+\frac{1}{2}}\}_{j=1}^3$ of the Roe matrix (3.13a) given by (omitting the subscript $(\cdot)_{\nu+\frac{1}{2}}$ of all averaged variables)

$$\widehat{\mathbf{r}}^1 = \begin{bmatrix} 1 \\ \bar{q} - \bar{c} \\ \bar{H} - \bar{q}\bar{c} \end{bmatrix}, \quad \widehat{\mathbf{r}}^2 = \begin{bmatrix} 1 \\ \bar{q} \\ \bar{q}^2/2 \end{bmatrix}, \quad \widehat{\mathbf{r}}^3 = \begin{bmatrix} 1 \\ \bar{q} + \bar{c} \\ \bar{H} + \bar{q}\bar{c} \end{bmatrix}, \tag{3.13c}$$

with the corresponding left eigenvector set $\{\widehat{\boldsymbol{\ell}}^j \equiv \widehat{\boldsymbol{\ell}}^j_{\nu+\frac{1}{2}}\}_{j=1}^3$ given by

$$\widehat{\boldsymbol{\ell}}^1 = \begin{bmatrix} \dfrac{(2+\widetilde{q})\widetilde{q}}{4(\gamma-1)} \\ -\dfrac{1+\widetilde{q}}{2\bar{c}} \\ \dfrac{\gamma-1}{2\bar{c}^2} \end{bmatrix}, \quad \widehat{\boldsymbol{\ell}}^2 = \begin{bmatrix} 1-\dfrac{\widetilde{q}^2}{2(\gamma-1)} \\ \dfrac{\widetilde{q}}{\bar{c}} \\ -\dfrac{\gamma-1}{\bar{c}^2} \end{bmatrix}, \quad \widehat{\boldsymbol{\ell}}^3 = \begin{bmatrix} -\dfrac{(2-\widetilde{q})\widetilde{q}}{4(\gamma-1)} \\ \dfrac{1-\widetilde{q}}{2\bar{c}} \\ \dfrac{\gamma-1}{2\bar{c}^2} \end{bmatrix}. \tag{3.13d}$$

Here $\widetilde{q} := (\gamma-1)\bar{q}/\bar{c}$, and $\bar{c}$ is the average sound speed given by $\bar{c}^2 = (\gamma-1)\big(\bar{H} - \frac{\bar{q}^2}{2}\big)$.

We are now able to form the intermediate path in $\mathbf{u}$-space as in (3.5)

$$\mathbf{u}^{j+1} = \mathbf{u}^j + \big\langle \widehat{\boldsymbol{\ell}}^j, \Delta\mathbf{u}\big\rangle \widehat{\mathbf{r}}^j, \quad j = 1,2,3. \tag{3.14}$$

Since the mapping between $\mathbf{u}$ and $\mathbf{v}$ is one-to-one, then these intermediate gridvalues in $\mathbf{u}$-space, $\{\mathbf{u}^j\}_{j=1}^4$, correspond to intermediate gridvalues $\{\mathbf{v}^j\}_{j=1}^4$ in $\mathbf{v}$-space. We let $\{\mathbf{r}^j\}_{j=1}^3$ be the (right) vectors connecting these $\mathbf{v}$-values, $\mathbf{r}^j := \mathbf{v}^{j+1} - \mathbf{v}^j$, and let $\{\boldsymbol{\ell}^j\}_{j=1}^3$ be the corresponding (left) orthogonal set. We summarize the algorithm of computing the entropy-conservative flux $\mathbf{f}^*_{\nu+\frac{1}{2}}$ in the following.

Algorithm 1. If $\mathbf{u}_\nu = \mathbf{u}_{\nu+1}$ **then** $\mathbf{f}^*_{\nu+\frac{1}{2}} = \mathbf{f}(\mathbf{v}_\nu)$; **else**

- Set $\mathbf{u}^1_{\nu+\frac{1}{2}} := \mathbf{u}_\nu$ and compute recursively the intermediate states,

$$\mathbf{u}^{j+1}_{\nu+\frac{1}{2}} = \mathbf{u}^j_{\nu+\frac{1}{2}} + \big\langle \widehat{\boldsymbol{\ell}}^j_{\nu+\frac{1}{2}}, \Delta\mathbf{u}_{\nu+\frac{1}{2}}\big\rangle \widehat{\mathbf{r}}^j_{\nu+\frac{1}{2}}, \quad j = 1,2,3. \tag{3.15}$$

  Here, $\{\widehat{\boldsymbol{\ell}}^j_{\nu+\frac{1}{2}}\}$ and $\{\widehat{\mathbf{r}}^j_{\nu+\frac{1}{2}}\}$ are the left and right eigensystems of the Roe matrix in (3.13c), (3.13d).
- Set $\mathbf{r}^j_{\nu+\frac{1}{2}} = \mathbf{v}(\mathbf{u}^{j+1}_{\nu+\frac{1}{2}}) - \mathbf{v}(\mathbf{u}^j_{\nu+\frac{1}{2}})$ and compute $\{\boldsymbol{\ell}^j\}_{j=1}^3$ as the corresponding orthogonal system,

$$\big\langle \boldsymbol{\ell}^j_{\nu+\frac{1}{2}}, \mathbf{r}^k_{\nu+\frac{1}{2}}\big\rangle = \delta_{jk}, \quad \mathbf{r}^j_{\nu+\frac{1}{2}} := \mathbf{v}^{j+1}_{\nu+\frac{1}{2}} - \mathbf{v}^j_{\nu+\frac{1}{2}} \tag{3.16}$$

- Compute the entropy-conservative numerical flux,

$$\mathbf{f}^*_{\nu+\frac{1}{2}} = \sum_{j=1}^{3} \frac{\psi\big(\mathbf{v}^{j+1}_{\nu+\frac{1}{2}}\big) - \psi\big(\mathbf{v}^j_{\nu+\frac{1}{2}}\big)}{\big\langle \boldsymbol{\ell}^j_{\nu+\frac{1}{2}}, \Delta\mathbf{v}_{\nu+\frac{1}{2}}\big\rangle} \boldsymbol{\ell}^j_{\nu+\frac{1}{2}}.$$

Remark 3.5. Observe that if $\{\mathbf{u}^{j+1} - \mathbf{u}^j\}_{j=1}^3$ are linearly independent then, since $\mathbf{u}_\mathbf{v}$ is symmetric positive definite, the corresponding set of directions in $\mathbf{v}$-phase space, $\{\mathbf{v}^{j+1} - \mathbf{v}^j\}_{j=1}^3$, are also linearly independent, at least when $\mathbf{u}_{\nu+1}$ is in a small neighborhood of $\mathbf{u}_\nu$. It guarantees the existence of the orthogonal set $\{\boldsymbol{\ell}^j\}_{j=1}^3$. But what happens when $\langle \hat{\boldsymbol{\ell}}^j, \Delta\mathbf{u}\rangle = 0$ for certain j's? For example, if $\mathbf{u}_\nu$ is connected to $\mathbf{u}_{\nu+1}$ through a k-shock, then the Roe matrix $[A]_{\nu+\frac{1}{2}}$ retains the perfect resolution of such a shock by enforcing $\langle \hat{\boldsymbol{\ell}}^j, \Delta\mathbf{u}\rangle = 0$, $\forall j \neq k$ and we can omit the contribution of these sub-paths to the conservative flux $\mathbf{f}^*$. The general approach is to construct a *precise* mirror image of the Roe-path in $\mathbf{v}$-phase space in terms of the right and left orthogonal systems,

$$\mathbf{r}^j := [H]^{-1}_{\nu+\frac{1}{2}}\hat{\mathbf{r}}^j, \quad \boldsymbol{\ell}^j := [H]_{\nu+\frac{1}{2}}\hat{\boldsymbol{\ell}}^j, \qquad j = 1, 2, \ldots, \tag{3.17}$$

where $[H]_{\nu+\frac{1}{2}}$ denotes an averaged symmetrizer such that $\Delta\mathbf{u}_{\nu+\frac{1}{2}} = [H]_{\nu+\frac{1}{2}}\Delta\mathbf{v}_{\nu+\frac{1}{2}}$ (and there are many such averages). Then, $\{\mathbf{r}^j\}_{j=1}^3$ forms the path in $\mathbf{v}$-phase space, $\mathbf{v}^{j+1} = \mathbf{v}^j + \langle \boldsymbol{\ell}^j, \Delta\mathbf{v}\rangle \mathbf{r}^j$, which retains the desired Roe property of perfect resolution of shocks. Indeed, if $\Delta\mathbf{u}$ is a k-shock with speed s then it satisfies (omitting subscripts) $\Delta\mathbf{f} = s\Delta\mathbf{u} = s[H]\Delta\mathbf{v}$. But the Roe matrix in (3.13a) is constructed so that [18], $\Delta\mathbf{f} = [A]\Delta\mathbf{u} = [A][H]\Delta\mathbf{v}$, and we conclude $\Delta\mathbf{v} = \mathbf{r}^k$. Thus, $\langle \boldsymbol{\ell}^j, \Delta\mathbf{v}\rangle = 0$, $\forall j \neq k$. The corresponding entropy conservative numerical flux reads

$$\mathbf{f}^*_{\nu+\frac{1}{2}} = \sum_{\{j|\xi^j\neq 0\}} \frac{\psi\big(\mathbf{v}^j_{\nu+\frac{1}{2}} + \xi^j \mathbf{r}^j_{\nu+\frac{1}{2}}\big) - \psi\big(\mathbf{v}^j_{\nu+\frac{1}{2}}\big)}{\xi^j} \boldsymbol{\ell}^j_{\nu+\frac{1}{2}}, \quad \xi^j = \big\langle \boldsymbol{\ell}^j_{\nu+\frac{1}{2}}, \Delta\mathbf{v}_{\nu+\frac{1}{2}}\big\rangle.$$

3.2.2. *The Navier–Stokes equations*

We turn to the construction of entropy-stable schemes for the full NS equations (1.1). To this end, we rewrite the equation as a system of conservation laws

$$\frac{\partial}{\partial t}\mathbf{u} + \frac{\partial}{\partial x}\mathbf{f}(\mathbf{u}) = \epsilon \frac{\partial^2}{\partial x^2}\mathbf{d}(\mathbf{u}), \qquad \mathbf{u} = \begin{bmatrix} \rho \\ m \\ E \end{bmatrix}, \quad \mathbf{f}(\mathbf{u}) = \begin{bmatrix} m \\ qm + p \\ q(E+p) \end{bmatrix}, \tag{3.18a}$$

with additional diffusive terms

$$\epsilon\mathbf{d}(\mathbf{u}) := (\lambda + 2\mu) \begin{bmatrix} 0 \\ q \\ q^2/2 \end{bmatrix} + \kappa \begin{bmatrix} 0 \\ 0 \\ \theta \end{bmatrix}. \tag{3.18b}$$

For the convection part on the left-hand side, we use the same entropy-conservative differencing used for the Euler equations. For the dissipative terms on the right-hand side, we employ standard centered differences. We arrive at our main result.

Theorem 3.6. *Let* (U, F) *be a given entropy pair of the NS equations* (3.18a), (3.18b), *which respect the entropy inequality* (2.10). *Consider the semi-discrete approximation*

$$\frac{d}{dt}\mathbf{u}_\nu(t) + \frac{1}{\Delta x_\nu}\big(\mathbf{f}^*_{\nu+\frac{1}{2}} - \mathbf{f}^*_{\nu-\frac{1}{2}}\big) = \frac{\epsilon}{\Delta x_\nu}\left(\frac{\mathbf{d}_{\nu+1} - \mathbf{d}_\nu}{\Delta x_{\nu+\frac{1}{2}}} - \frac{\mathbf{d}_\nu - \mathbf{d}_{\nu-1}}{\Delta x_{\nu-\frac{1}{2}}}\right). \tag{3.19a}$$

Here $\mathbf{f}^*_{\nu+\frac{1}{2}}$ *is an entropy conservative numerical flux* (3.7),

$$\mathbf{f}^*_{\nu+\frac{1}{2}} = \sum_{j=1}^{3} \frac{\psi\big(\mathbf{v}^{j+1}_{\nu+\frac{1}{2}}\big) - \psi\big(\mathbf{v}^j_{\nu+\frac{1}{2}}\big)}{\big\langle \boldsymbol{\ell}^j_{\nu+\frac{1}{2}}, \Delta\mathbf{v}_{\nu+\frac{1}{2}}\big\rangle} \boldsymbol{\ell}^j_{\nu+\frac{1}{2}}, \tag{3.19b}$$

which is outlined in Algorithm 1 *above.*

{i} *The resulting scheme* (3.19a), (3.19b) *is entropy-dissipative in the sense that*

$$\frac{d}{dt}\sum_\nu U_\nu(t)\,\Delta x_\nu = -\sum_\nu \frac{\epsilon}{\Delta x_{\nu+\frac{1}{2}}}\left\langle \Delta\mathbf{v}_{\nu+\frac{1}{2}},\, \frac{\Delta\mathbf{d}_{\nu+\frac{1}{2}}}{\Delta\mathbf{v}_{\nu+\frac{1}{2}}}\Delta\mathbf{v}_{\nu+\frac{1}{2}}\right\rangle \leq 0. \tag{3.20}$$

This entropy balance is a discrete analogue of the entropy balance statements (2.15) *and* (2.17).

{ii} *In the specific case of the canonical entropy pair* $(U,F)=(-\rho S,-mS)$, *the entropy decay* (3.20) *amounts to* (1.11)

$$\begin{aligned}\frac{d}{dt}\sum_\nu U_\nu(t)\Delta x_\nu &= -(\lambda+2\mu)\sum_\nu\left(\frac{\Delta q_{\nu+\frac{1}{2}}}{\Delta x_{\nu+\frac{1}{2}}}\right)^2 \widehat{(1/\theta)}_{\nu+\frac{1}{2}}\Delta x_{\nu+\frac{1}{2}}\\ &\quad -\kappa\sum_\nu\left(\frac{\Delta\theta_{\nu+\frac{1}{2}}}{\Delta x_{\nu+\frac{1}{2}}}\right)^2 \widetilde{(1/\theta)}^2_{\nu+\frac{1}{2}}\Delta x_{\nu+\frac{1}{2}} \leq 0. \end{aligned}\tag{3.21}$$

Proof. We multiply (3.19a) by $[U_{\mathbf{u}}]_\nu^\top = \mathbf{v}_\nu^\top$, then sum up all spatial cells to get the balance of the total entropy,

$$\frac{d}{dt}\sum_\nu U_\nu(t)\Delta x_\nu + \sum_\nu\left\langle \mathbf{v}_\nu,\, \mathbf{f}^*_{\nu+\frac{1}{2}} - \mathbf{f}^*_{\nu-\frac{1}{2}}\right\rangle = \epsilon\sum_\nu\left\langle \mathbf{v}_\nu,\, \frac{\mathbf{d}_{\nu+1}-\mathbf{d}_\nu}{\Delta x_{\nu+\frac{1}{2}}} - \frac{\mathbf{d}_\nu-\mathbf{d}_{\nu-1}}{\Delta x_{\nu-\frac{1}{2}}}\right\rangle. \tag{3.22}$$

Since we chose $\mathbf{f}^*_{\nu+\frac{1}{2}}$ as the entropy conservative flux, a straightforward manipulation on the entropy conservation requirement (3.8) yields the conservative difference,

$$\left\langle \mathbf{v}_\nu, \mathbf{f}^*_{\nu+\frac{1}{2}} - \mathbf{f}^*_{\nu-\frac{1}{2}}\right\rangle = F_{\nu+\frac{1}{2}} - F_{\nu-\frac{1}{2}}, \tag{3.23}$$

where $2F_{\nu+\frac{1}{2}} = \left\langle(\mathbf{v}_\nu+\mathbf{v}_{\nu+1}), \mathbf{f}_{\nu+\frac{1}{2}}\right\rangle - (\psi(\mathbf{v}_\nu)+\psi(\mathbf{v}_{\nu+1}))$. On the other hand, summation by parts on the right-hand side of (3.22) yields

$$\begin{aligned}\epsilon\sum_\nu&\left\langle \mathbf{v}_\nu,\, \frac{\mathbf{d}_{\nu+1}-\mathbf{d}_\nu}{\Delta x_{\nu+\frac{1}{2}}} - \frac{\mathbf{d}_\nu-\mathbf{d}_{\nu-1}}{\Delta x_{\nu-\frac{1}{2}}}\right\rangle \Delta x_{\nu+\frac{1}{2}}\\ &= -\sum_\nu \frac{\epsilon}{\Delta x_{\nu+\frac{1}{2}}}\left\langle \Delta\mathbf{v}_{\nu+\frac{1}{2}},\, \Delta\mathbf{d}_{\nu+\frac{1}{2}}\right\rangle &\text{(3.24a)}\\ &= -\sum_\nu \frac{\epsilon}{\Delta x_{\nu+\frac{1}{2}}}\left\langle \Delta\mathbf{v}_{\nu+\frac{1}{2}},\, \frac{\Delta\mathbf{d}_{\nu+\frac{1}{2}}}{\Delta\mathbf{v}_{\nu+\frac{1}{2}}}\Delta\mathbf{v}_{\nu+\frac{1}{2}}\right\rangle. &\text{(3.24b)}\end{aligned}$$

By (3.23) and (3.24b), the semi-discrete entropy balance amounts to

$$\frac{d}{dt}\sum_\nu U_\nu(t)\Delta x_\nu = -\sum_\nu \frac{\epsilon}{\Delta x_{\nu+\frac{1}{2}}}\left\langle \Delta\mathbf{v}_{\nu+\frac{1}{2}},\, \frac{\Delta\mathbf{d}_{\nu+\frac{1}{2}}}{\Delta\mathbf{v}_{\nu+\frac{1}{2}}}\Delta\mathbf{v}_{\nu+\frac{1}{2}}\right\rangle. \tag{3.25}$$

Here

$$\frac{\Delta\mathbf{d}_{\nu+\frac{1}{2}}}{\Delta\mathbf{v}_{\nu+\frac{1}{2}}} = \int_{\xi=-\frac{1}{2}}^{\frac{1}{2}} \mathbf{d}_{\mathbf{v}}\left(\mathbf{v}_{\nu+\frac{1}{2}}(\xi)\right)d\xi,$$

where $\mathbf{v}_{\nu+\frac{1}{2}}(\xi)$ is given by (3.12). By the admissibility of the dissipative NS fluxes $\mathbf{d}_{\mathbf{v}} \geq 0$ and the right-hand side of (3.25) is indeed non-positive. Thus, the semi-discrete scheme (3.19a) guarantees the total entropy dissipation.

In the specific case of the entropy pair $(U, F) = (-\rho S, -mS)$, the entropy variable are found in (2.14), and we explicitly compute the inner products in (3.24a) as (omitting all subscripts),

$$
\begin{aligned}
-\sum_\nu & \frac{\epsilon}{\Delta x} \langle \Delta \mathbf{v}, \, \Delta \mathbf{d} \rangle \\
&= -\sum_\nu \frac{1}{\Delta x} \left\{ (\lambda + 2\mu) \Delta \left(\frac{q}{\theta}\right) \Delta q - \frac{\lambda + 2\mu}{2} \Delta \left(\frac{1}{\theta}\right) \Delta \big(q^2\big) - \kappa \, \Delta \left(\frac{1}{\theta}\right) \Delta \theta \right\} \\
&= -(\lambda + 2\mu) \sum_\nu \frac{1}{\Delta x} (\Delta q)^2 \frac{1}{2} \left(\frac{1}{\theta_{\nu+1}} + \frac{1}{\theta_\nu} \right) - \kappa \sum_\nu \frac{1}{\Delta x} \Delta \left(\frac{1}{\theta}\right) \Delta \theta \\
&= -(\lambda + 2\mu) \sum_\nu \left(\frac{\Delta q}{\Delta x} \right)^2 \frac{1}{2} \left(\frac{1}{\theta_{\nu+1}} + \frac{1}{\theta_\nu} \right) \Delta x - \kappa \sum_\nu \left(\frac{\Delta \theta}{\Delta x} \right)^2 \frac{1}{\theta_{\nu+1} \theta_\nu} \Delta x \leq 0.
\end{aligned}
$$

The discrete entropy balance (1.11) now follows. □

We emphasize the main point made here, namely, we introduce no excessive entropy dissipation due to spurious, *artificial* numerical viscosity: by (3.20), the semi-discrete scheme contains the precise amount of numerical viscosity to enforce the correct entropy dissipation dictated by the NS equations.

3.3. *Time discretization*

To complete the computation of a semi-discrete scheme, it needs to be augmented with a proper time discretization. To enable a large time-stability region and maintain simplicity, the three-stage third-order Runge–Kutta (RK3) method will be used, consult [3],

$$
\mathbf{u}_\nu(t^n + \Delta t) = \mathbf{u}_\nu(t^n) - \frac{\Delta t}{9} (2K_{\nu,1} + 3K_{\nu,2} + 4K_{\nu,3}), \tag{3.26}
$$

where

$$
\begin{cases}
K_{\nu,1} = \dfrac{-1}{\Delta x_\nu} \left\{ \mathbf{f}^*_{\nu+\frac{1}{2}} \big(\mathbf{u}^n_\nu, \mathbf{u}^n_{\nu+1}\big) - \mathbf{f}^*_{\nu-\frac{1}{2}} \big(\mathbf{u}^n_{\nu-1}, \mathbf{u}^n_\nu\big) \right\}, \\[2ex]
K_{\nu,2} = \dfrac{-1}{\Delta x_\nu} \left\{ \mathbf{f}^*_{\nu+\frac{1}{2}} \left(\mathbf{u}^n_\nu + \dfrac{\Delta t}{2} K_{\nu,1}, \mathbf{u}^n_{\nu+1} + \dfrac{\Delta t}{2} K_{\nu+1,1} \right) \right. \\
\qquad\qquad \left. - \, \mathbf{f}^*_{\nu-\frac{1}{2}} \left(\mathbf{u}^n_{\nu-1} + \dfrac{\Delta t}{2} K_{\nu-1,1}, \mathbf{u}^n_\nu + \dfrac{\Delta t}{2} K_{\nu,1} \right) \right\}, \\[2ex]
K_{\nu,3} = \dfrac{-1}{\Delta x_\nu} \left\{ \mathbf{f}^*_{\nu+\frac{1}{2}} \left(\mathbf{u}^n_\nu + \dfrac{3\Delta t}{4} K_{\nu,2}, \mathbf{u}^n_{\nu+1} + \dfrac{3\Delta t}{4} K_{\nu+1,2} \right) \right. \\
\qquad\qquad \left. - \, \mathbf{f}^*_{\nu-\frac{1}{2}} \left(\mathbf{u}^n_{\nu-1} + \dfrac{3\Delta t}{4} K_{\nu-1,2}, \mathbf{u}^n_\nu + \dfrac{3\Delta t}{4} K_{\nu,2} \right) \right\}.
\end{cases}
$$

The resulting fully-discrete schemes has a spatial stencil involving seven-point grid-values, with two "ghost" boundary values on the left boundary and two "ghost" boundary on the right required to close the system. For simplicity, these "ghost" values are extrapolated from the given Dirichlet boundary values. We note in passing that though the fully explicit RK3 time discretization need not conserve the entropy, it introduces a negligible amount of entropy dissipation; for a general framework of entropy-conservative fully discrete schemes consult [13].

4. Numerical Experiments

We consider ideal polytropic gas equations as an approximation of air with

$$\gamma = 1.4, \quad C_v = 716, \quad \kappa = 0.03, \quad \lambda + 2\mu = 2.28 \times 10^{-5}.$$

We simulate the Sod's shocktube problem, [19], where the Euler and NS equations are solved over the interval [0, 1] subject to Riemann initial conditions

$$\big(\rho, m, E\big)_{t=0} = \begin{cases} (1.0, 0.0, 2.5), & 0 < x \leq 0.5, \\ (0.125, 0.0, 0.25), & 0.5 < x < 1. \end{cases}$$

In the following figures, we display the numerical solutions for the fully discrete scheme (3.26) with the numerical flux (3.7), or in its equivalent yet simpler form (3.11). Uniform space and time grid sizes, Δx and Δt, are used. Both viscous and inviscid cases are explored. We use different spatial resolutions for the same problem, and adjust time step according to the CFL condition. Different choices of entropy function are also tested in the numerical experiments. We group our results into four sets.

1. Euler equations. The first four sets of figures are devoted to the Euler equations with zero viscous and heat fluxes (1.5).

With the choice of the entropy pair

$$(U(\mathbf{u}),\, F(\mathbf{u})) = \left(\frac{1+\gamma}{1-\gamma} (\rho p)^{\frac{1}{1+\gamma}},\, \frac{1+\gamma}{1-\gamma} q (\rho p)^{\frac{1}{1+\gamma}} \right), \tag{4.1}$$

Fig. 1 depicts the density, velocity, and pressure fields at $t = 0.05$ and $t = 0.1$; here we use $\Delta x = 0.001$ and $\frac{\Delta t}{\Delta x} = 0.025$. Comparing these to the corresponding results of the canonical entropy pair

$$(U(\mathbf{u}),\, F(\mathbf{u})) = \left(-\rho \ln(p\rho^{-\gamma}), -m \ln(p\rho^{-\gamma})\right), \tag{4.2}$$

in Fig. 2, we see that the different choices of entropies do not affect the behavior of the numerical solutions. Figures 1(d) and 2(d) demonstrate the conservation of the total entropies: the negligible amount of entropy decay $\sim 10^{-4}$ is introduced by the RK3 time discretization.

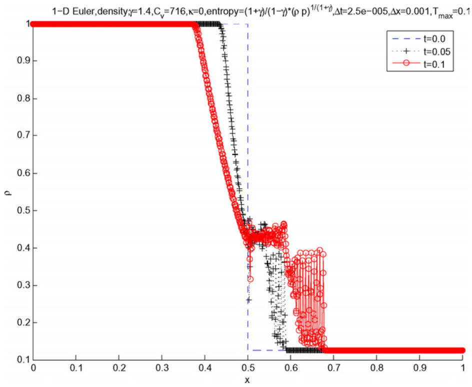

(a) Density

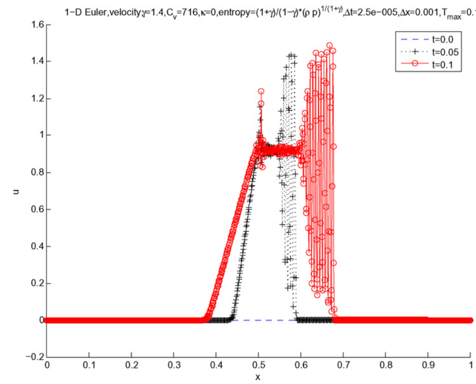

(b) Velocity

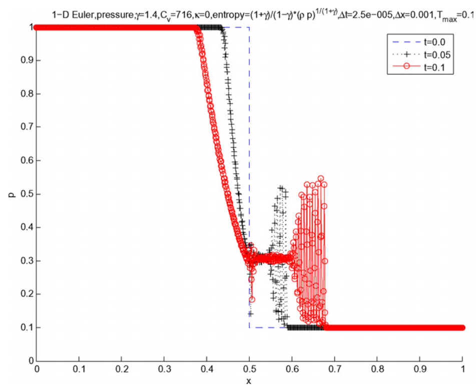

(c) Pressure

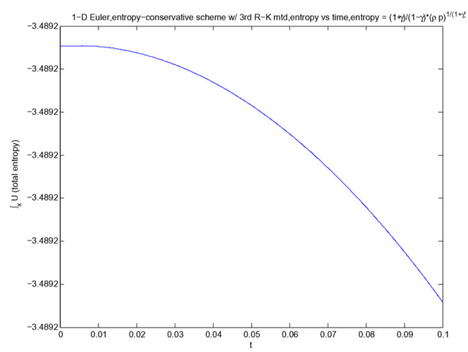

(d) Total entropy vs. time

Fig. 1. Euler equations with 1,000 spatial gridpoints, $U(\mathbf{u}) = \frac{1+\gamma}{1-\gamma} \cdot (p\rho)^{\frac{1}{1+\gamma}}$, $\Delta t = 2.5 \times 10^{-5}$, $\Delta x = 10^{-3}$.

Next, we make the same comparison for the refined the spatial mesh, taking $\Delta x = 0.00025$, $\frac{\Delta t}{\Delta x} = 0.1$. Figure 3 presents the computed solutions of density, velocity, and pressure fields at $t = 0.05$ and $t = 0.1$ with the entropy pair (4.1) while Fig. 4 depicts the solutions with the canonical entropy pair (4.2). The total entropy is shown in Figs. 3(d) and 4(d).

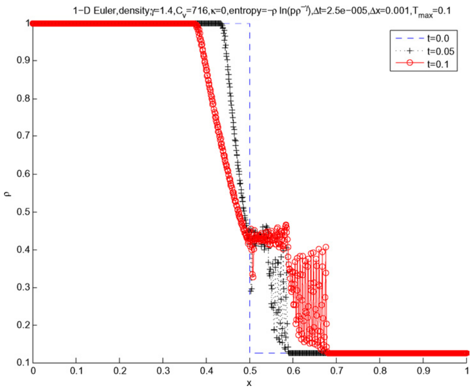

(a) Density

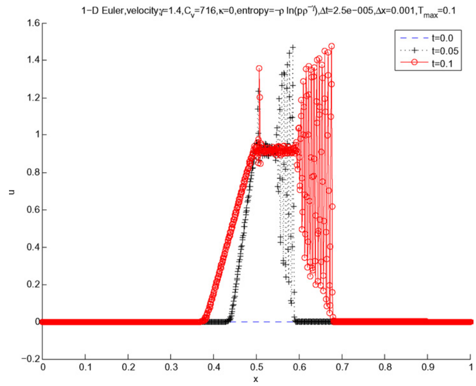

(b) Velocity

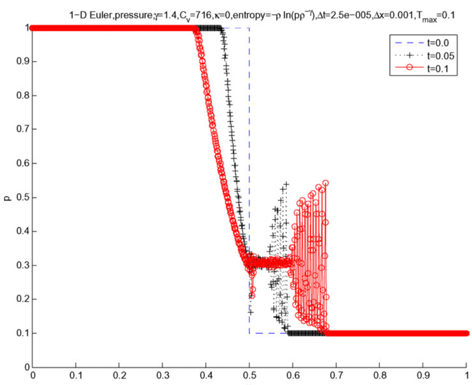

(c) Pressure

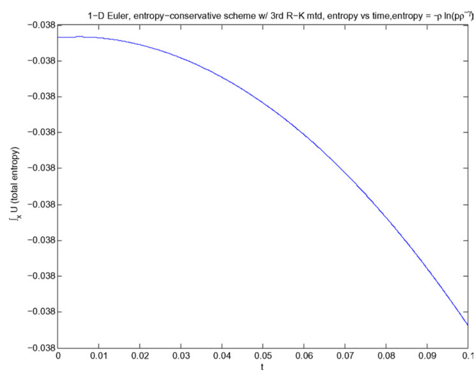

(d) Total entropy vs. time

Fig. 2. Euler equations with 1,000 spatial gridpoints, $U(\mathbf{u}) = -\rho \ln\big(p\rho^{-\gamma}\big)$ and same Δt and Δx as Fig. 1.

The above results demonstrate the purely dispersive character of the entropy conservative schemes. Dispersive oscillations on the mesh scale are observed in shocks and contact regions, due to the absence of any dissipation mechanism, consult [11, 15]. The numerical solutions do *not* blow up. Actually, as we refine the mesh, these dispersive oscillations approach a modulated wave envelope. The study

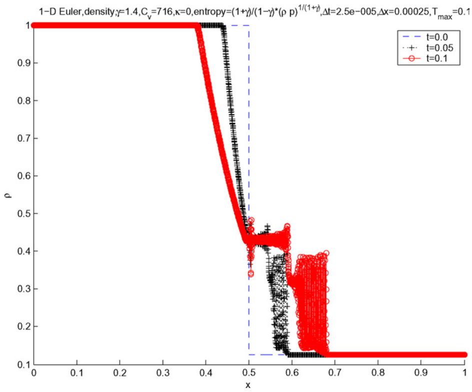

(a) Density

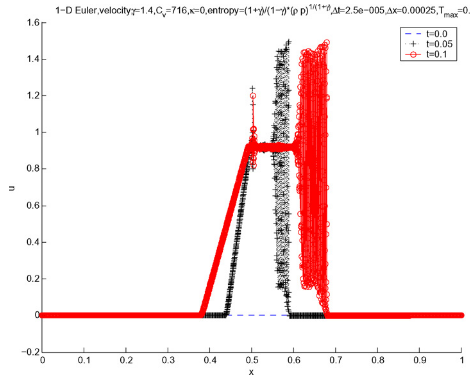

(b) Velocity

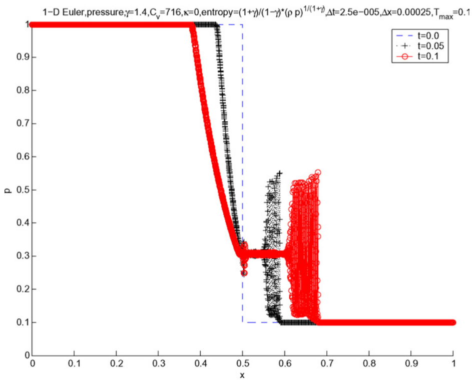

(c) Pressure

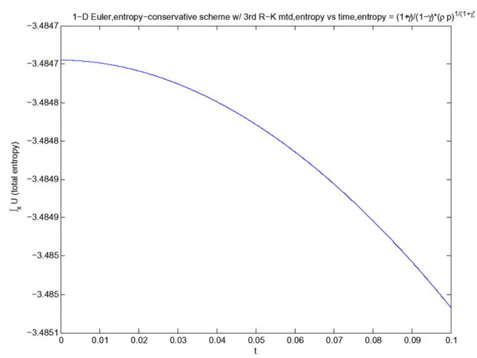

(d) Total entropy vs. time

Fig. 3. Euler equations with 4,000 spatial gridpoints, $U(\mathbf{u}) = \frac{1+\gamma}{1-\gamma} \cdot (p\rho)^{\frac{1}{1+\gamma}}$, $\Delta t = 2.5 \times 10^{-5}$, $\Delta x = 2.5 \times 10^{-4}$.

of these modulated waves in the conservative Euler equations would be an extremely challenging task. A similar entropy conservative *Lagrangian formulation* of Euler equations of [25] motivated the discussion in [11].

2. Navier–Stokes equations with heat flux. We solve the Navier–Stokes equations (1.4). The results are summarized in the next three sets of Figs. 5–7.

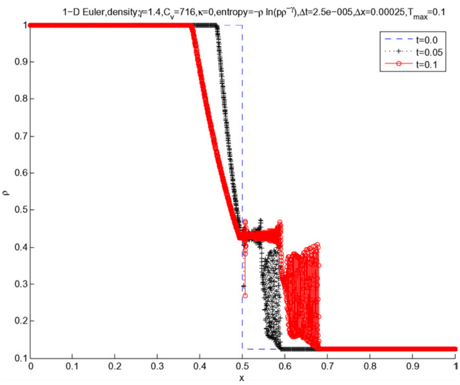

(b) Velocity

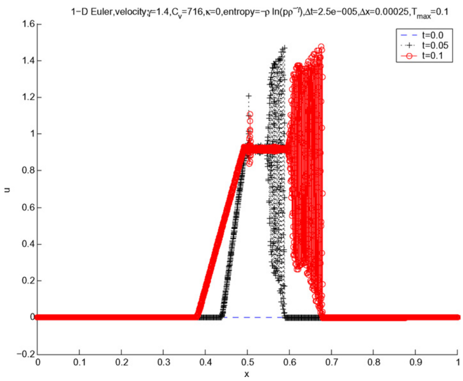

(a) Density

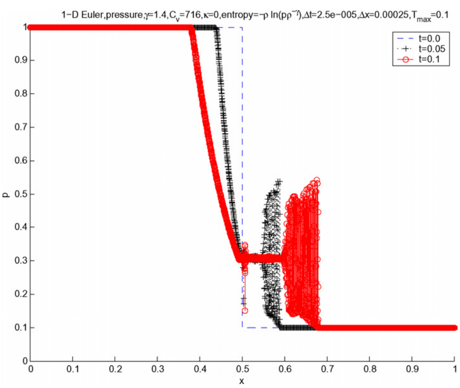

(c) Pressure

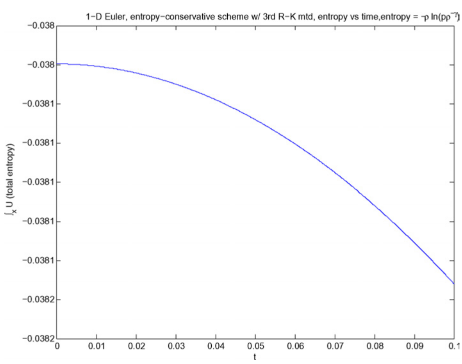

(d) Total entropy vs. time

Fig. 4. Euler equations with 4,000 spatial gridpoints, $U(\mathbf{u}) = -\rho\ln\bigl(p\rho^{-\gamma}\bigr)$ and same Δt and Δx as Fig. 3.

We follow the same pattern of plotting density, velocity, pressure and total entropy. As before, the choice of entropy pairs (4.1) in Figs. 5 and 6 are very similar.

The presence of heat flux causes the oscillations to be dramatically reduced around the contact discontinuity. Furthermore, oscillations are significantly damped around the shock; when the mesh is well-refined, Fig. 7 shows that heat conduction

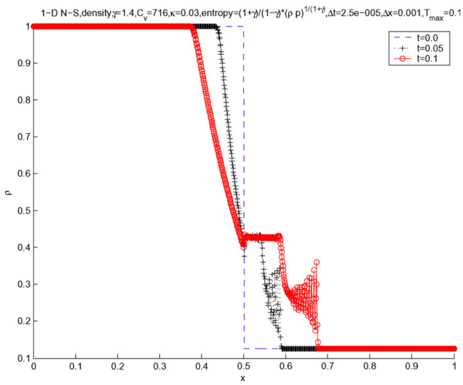

(a) Density

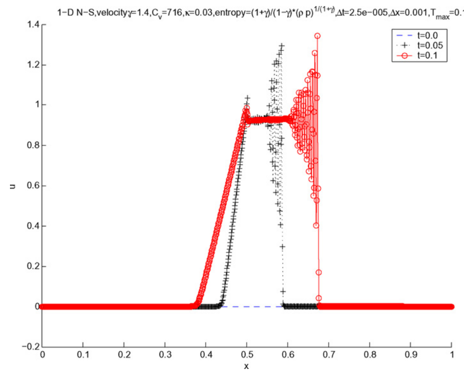

(b) Velocity

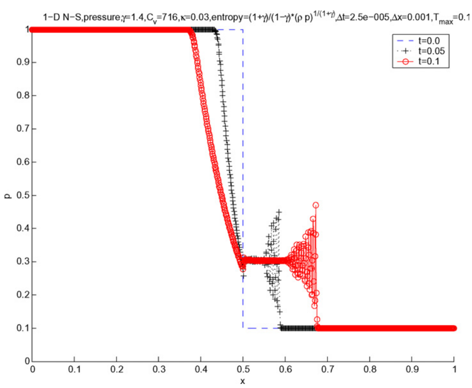

(c) Pressure

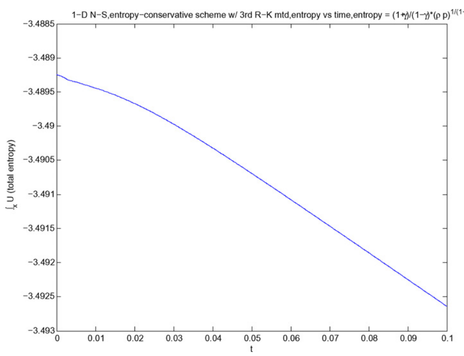

(d) Total entropy vs. time

Fig. 5. Navier–Stokes equations with heat conduction and no viscous term. 1,000 spatial gridpoints, $U(\mathbf{u}) = \frac{1+\gamma}{1-\gamma} \cdot (p\rho)^{\frac{1}{1+\gamma}}$, $\Delta t = 2.5 \times 10^{-5}$, $\Delta x = 10^{-3}$.

causes these oscillations to be well localized in the immediate neighborhood of the shocks. If the mesh is underresolved, a small portion of dispersive oscillations persist in the neighborhood of shocks.

3. Navier–Stokes equations with viscosity and no heat flux. We solve the viscous NS equations (1.3). The results are summarized in Figs. 8–9. Since the

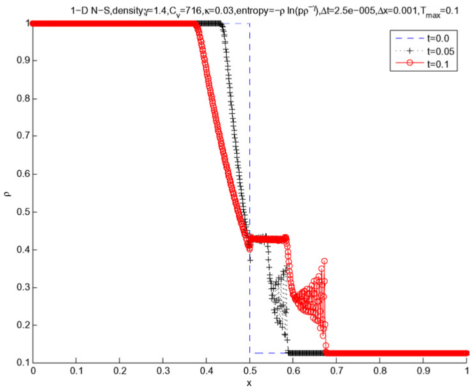

(a) Density

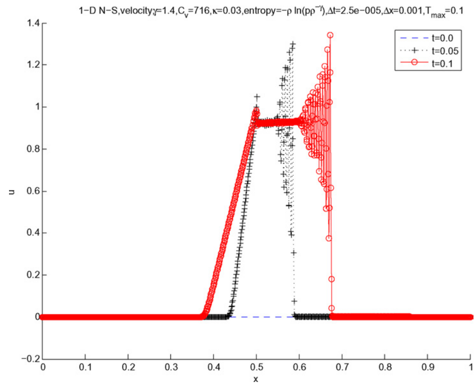

(b) Velocity

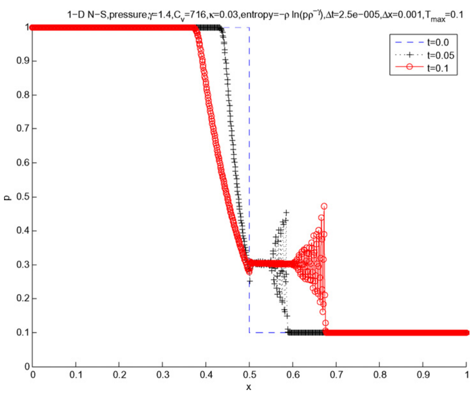

(c) Pressure

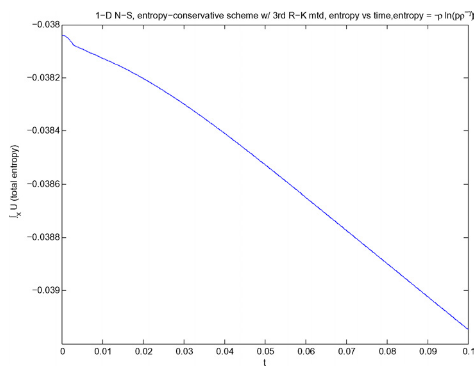

(d) Total entropy vs. time

Fig. 6. Navier–Stokes equations with heat conduction and no viscous terms. 1,000 spatial grid-points, $U(\mathbf{u}) = -\rho \ln\left(p\rho^{-\gamma}\right)$ and same Δt and Δx as Fig. 5.

results are essentially independent of the choice of entropy, we chose to quote here only the results for the canonical pair (4.2).

The viscosity in NS equations is doing a better job than heat flux in damping oscillations around the shock discontinuity. The plots of total entropy, reveal a greater entropy decay than the NS equations with heat conduction. On the other

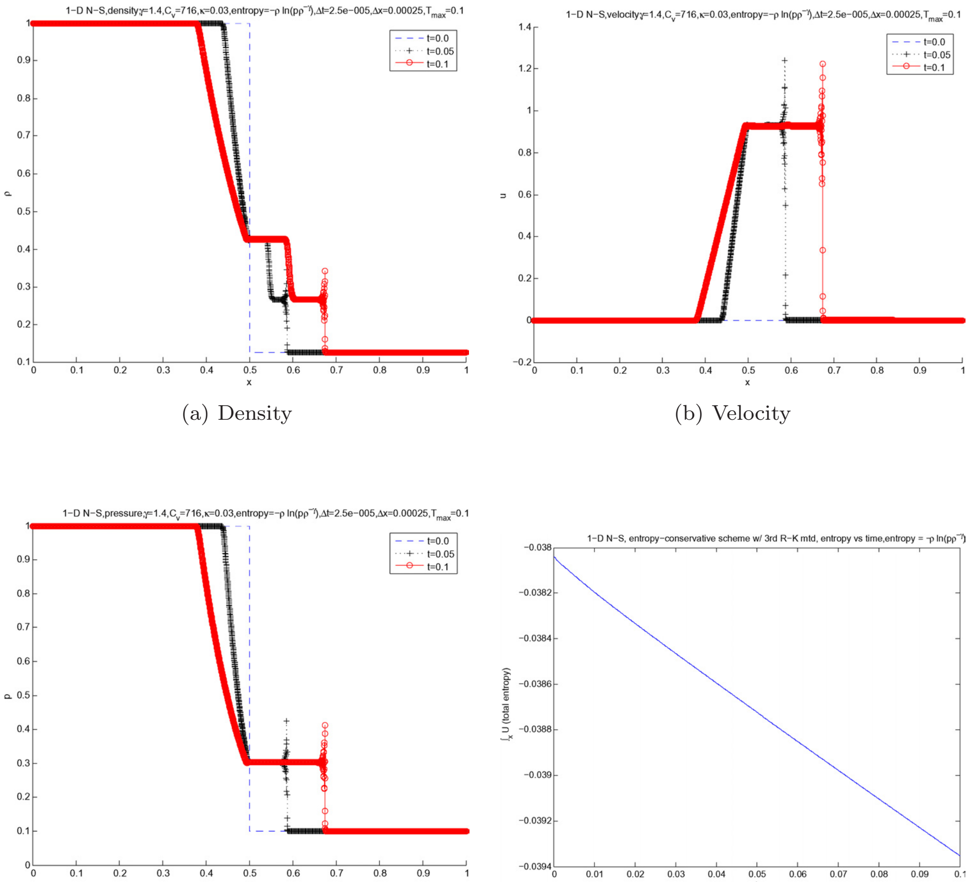

(a) Density (b) Velocity

(c) Pressure (d) Total entropy vs. time

Fig. 7. Navier–Stokes equations with heat conduction and no viscous terms. 4,000 spatial grids, $U(\mathbf{u}) = -\rho \ln\big(p\rho^{-\gamma}\big)$, $\Delta t = 2.5 \times 10^{-5}$, $\Delta x = 2.5 \times 10^{-4}$.

hand, we still observe an oscillatory behavior around the contact discontinuity, even with the refined mesh in Fig. 9.

4. Full Navier–Stokes equations with viscous and heat fluxes. In Figs. 10–11, we record the results for the full NS equations (1.1). As before, the difference

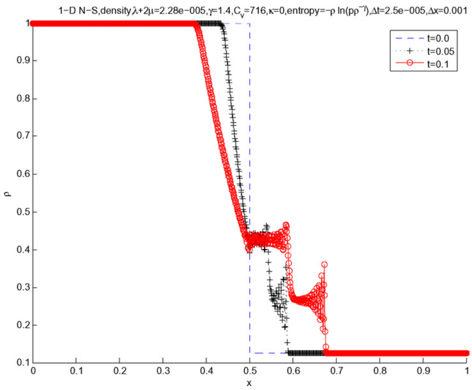

(a) Density

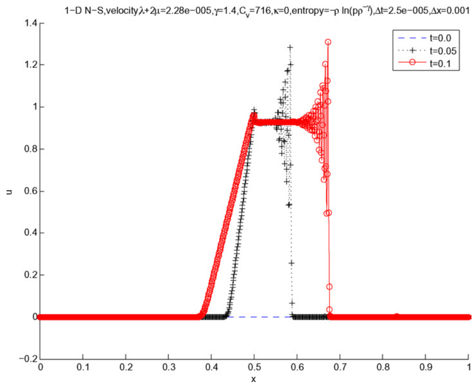

(b) Velocity

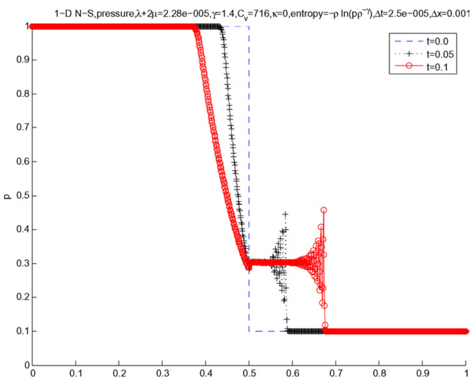

(c) Pressure

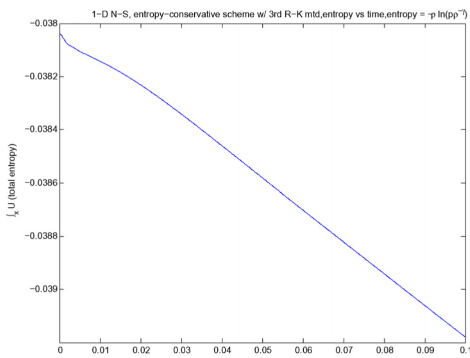

(d) Total entropy vs. time

Fig. 8. Navier–Stokes equations with viscous terms and no heat conduction. 1,000 spatial grid-points, $U(\mathbf{u}) = -\rho \ln\big(p\rho^{-\gamma}\big)$, $\Delta t = 2.5 \times 10^{-5}$, $\Delta x = 10^{-3}$.

due to different entropy functions is undetectable and we chose to record here only the canonical entropy.

As expected, these numerical solutions are the smoothest ones found in our numerical experiments, especially with very fine meshes, depicted in Fig. 11. Small oscillations remain with underresolved meshes.

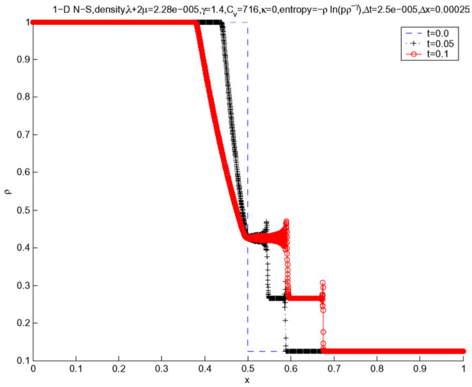

(a) Density

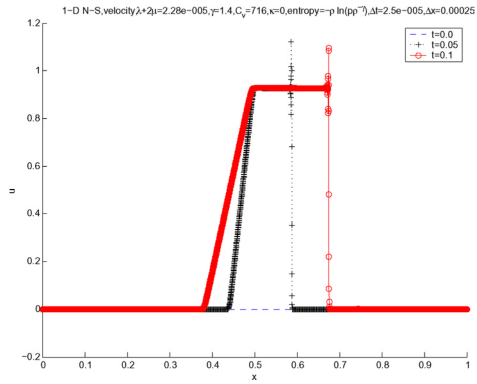

(b) Velocity

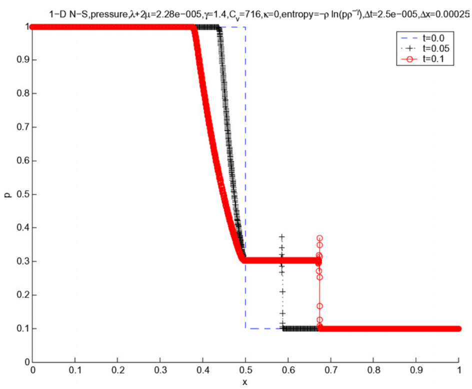

(c) Pressure

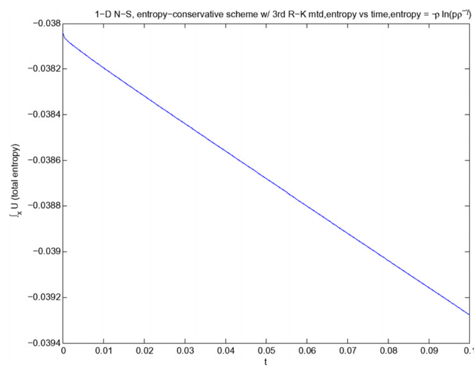

(d) Total entropy vs. time

Fig. 9. Navier–Stokes equations with viscous terms and no heat conduction. 4,000 spatial grids, $U(\mathbf{u}) = -\rho \ln\left(p\rho^{-\gamma}\right)$, $\Delta t = 2.5 \times 10^{-5}$, $\Delta x = 2.5 \times 10^{-4}$.

Not only the oscillations around the shocks are damped out by viscosity, but the oscillations around the contact discontinuity are significantly reduced due to the heat flux. Compared with the results of NS equations with heat conduction (1.4) in Figs. 6–7, oscillations in the neighborhood of the shock are better damped

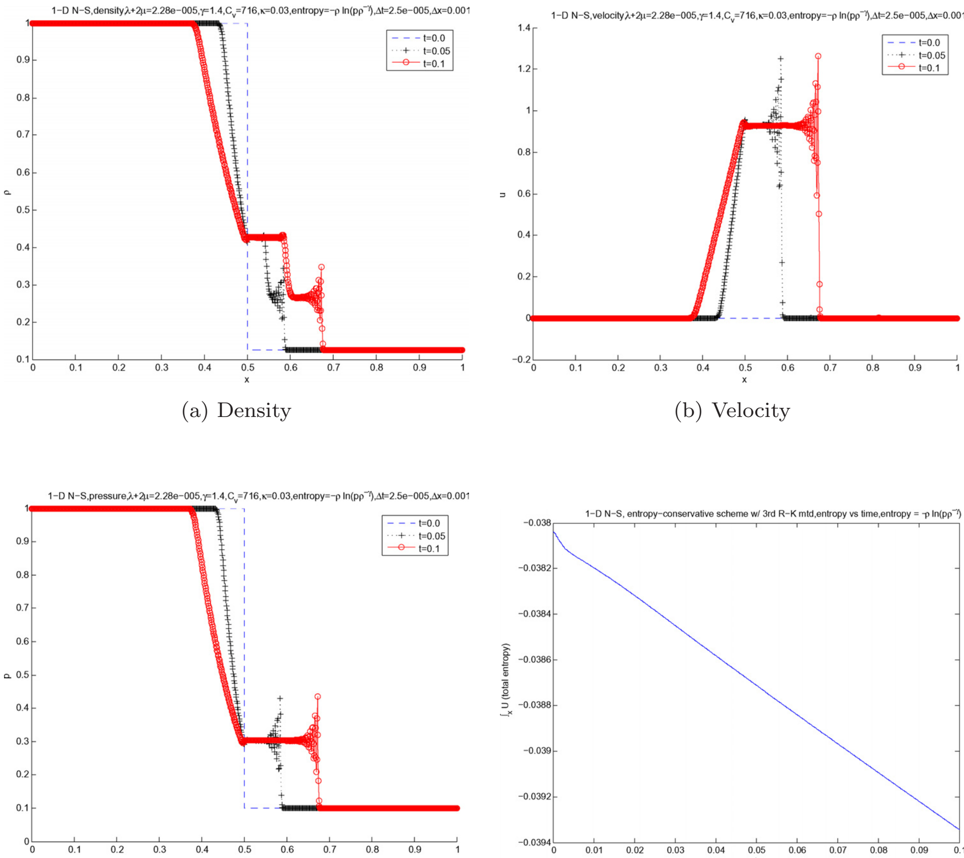

(a) Density

(b) Velocity

(c) Pressure

(d) Total entropy vs. time

Fig. 10. Navier–Stokes equations with viscosity and heat conduction. 1,000 spatial gridpoints, $U(\mathbf{u}) = -\rho \ln\big(p\rho^{-\gamma}\big)$, $\Delta t = 2.5 \times 10^{-5}$, $\Delta x = 10^{-3}$.

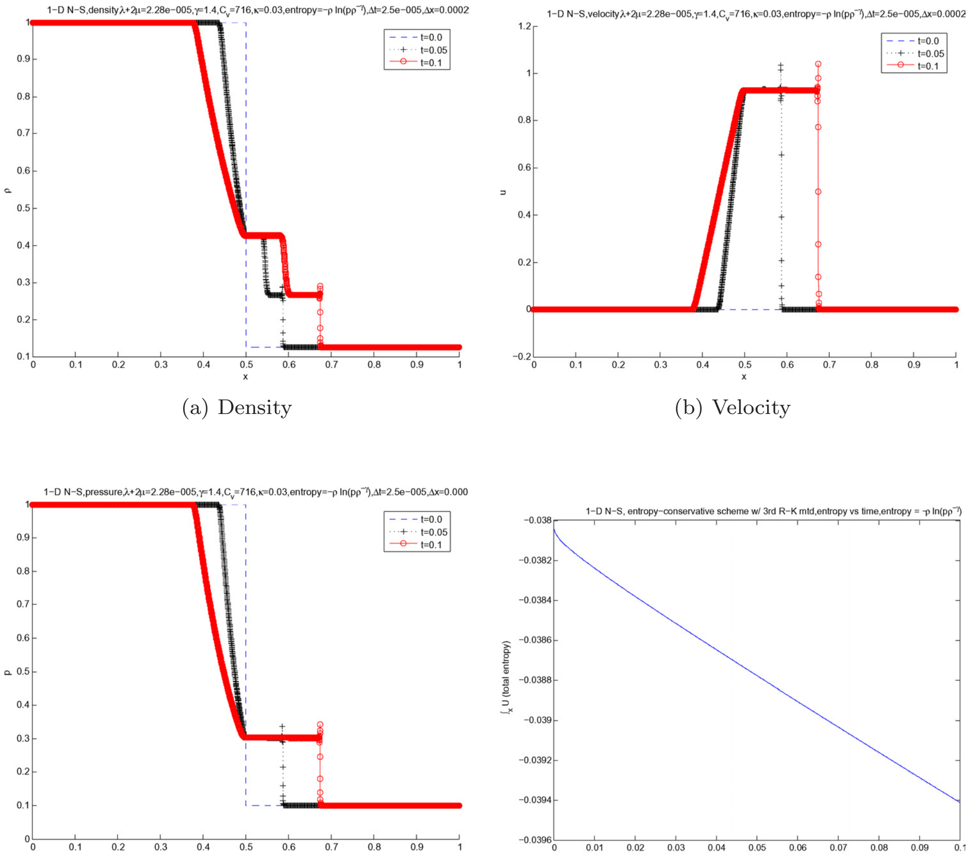

(a) Density

(b) Velocity

(c) Pressure

(d) Total entropy vs. time

Fig. 11. Navier–Stokes equations with viscosity and heat conduction. 4,000 spatial gridpoints, $U(\mathbf{u}) = -\rho \ln(p\rho^{-\gamma})$, $\Delta t = 2.5 \times 10^{-5}$, $\Delta x = 2.5 \times 10^{-4}$.

here thanks to the viscosity terms. The remaining sharp "spike" at the tip of shock discontinuity is due to the relatively small viscosity coefficient of air.

Acknowledgment

Weigang Zhong wants to thank Ning Jiang, Dongming Wei, and Bin Cheng for their very intriguing discussions. Research was supported in part by NSF DMS #DMS04-07704 and ONR #N00014-91-J-1076.

References

[1] C. Dafermos, *Hyperbolic Conservation Laws in Continuum Mechanics* (Springer, 2000).
[2] S. K. Godunov, An interesting class of quasilinear systems, *Dokl. Acad. Nauk. SSSR* **139** (1961) 521–523.
[3] S. Gottlieb, C.-W. Shu and E. Tadmor, Strong stability-preserving high-order time discretization methods, *SIAM Rev.* **43**(1) (2001) 89–112.
[4] S. R. de Groot and P. Mazur, *Non-Equilibrium Thermodynamics* (Dover, 1984).
[5] A. Harten, On the symmetric form of systems of conservation laws with entropy, *J. Comput. Phys.* **49** (1983) 151–164.
[6] T. J. R. Hughes, L. P. Franca and M. Mallet, A new finite element formulation for computational fluid dynamics: I. Symmetric forms of the compressible Euler and Navier-stokes equations and the second law of thermodynamics, *Comput. Methods Appl. Mech. Eng.* **54** (1986) 223–234.
[7] M. Mallet, A new finite element formulation for computational fluid dynamics: III. The generalized streamline operator for multidimensional advective-diffusive systems, *Comput. Methods Appl. Mech. Eng.* **58**(3) (1986) 305–328.
[8] M. Mallet, A new finite element formulation for computational fluid dynamics: IV. A discontinuity- capturing operator for multidimensional advective-diffusive systems, *Comput. Methods Appl. Mech. Eng.* **58**(3) (1986) 329–336.
[9] M. Mallet and A. Mizukami, A new finite element formulation for computational fluid dynamics: II. Beyond SUPG, *Comput. Methods Appl. Mech. Eng.* **54**(3) (1986) 341–355.
[10] P. D. Lax, *Hyperbolic Systems of Conservation Laws and the Mathematical Theory of Shock Waves*, CBMS-NSF, Vol. 11 (SIAM, 1973).
[11] P. D. Lax, On dispersive difference schemes, *Phys. D* **18** (1986) 250–254.
[12] P. D. Lax, C. D. Levermore and S. Venakides, The generation and propagation of oscillations in dispersive IVPs and their limiting behavior, in *Important Developments in Soliton Theory 1980–1990*, eds. T. Fokas and V. E. Zakharov (Springer-Verlag, 1993).
[13] P. G. LeFloch, J. M. Mercier and C. Rohde, Full discrete, entropy conservative schemes of arbitrary order, *SIAM J. Numer. Anal.* **40**(5) (2002) 1968–1992.
[14] P. G. LeFloch and C. Rohde, High-order schemes, entropy inequalities, and nonclassical shocks, *SIAM J. Numer. Anal.* **37**(6) (2000) 2023–2060.
[15] C. D. Levermore and J.-G. Liu, Oscillations arising in numerical experiments, *Phys. D* **99** (1996) 191–216.
[16] T.-P. Liu, Viscosity criterion for hyperbolic conservation laws, in *Viscous Profiles and Numerical Methods for Shock Wave*, ed. M. Shearer (SIAM, 1991), pp. 105–114.
[17] M. S. Mock, Systems of conservation of mixed type, *J. Differential Equations* **37** (1980) 70–88.

[18] P. L. Roe, Approximate Riemann solvers, parameter vectors and difference schemes, *J. Comput. Phys.* **43** (1981) 357–372.
[19] G. Sod, A survey of several difference methods for hyperbolic systems of nonlinear conservation laws, *J. Comput. Phys.* **27** (1978) 1–31.
[20] E. Tadmor, Skew-selfadjoint form for systems of conservation laws, *J. Math. Anal. Appl.* **103** (1984) 428–442.
[21] E. Tadmor, Numerical viscosity and the entropy condition for conservative difference schemes, *Math. Comput.* **43** (1984) 369–381.
[22] E. Tadmor, Entropy conservative finite element schemes, in *Numerical Methods for Compressible Flows — Finite Difference Element and Volume Techniques, Proc. Winter Annual Meeting of the ASME*, eds. T. E. Tezduyar and T. J. R. Hughes, AMD, Vol. 78 (1986), pp. 149–158.
[23] E. Tadmor, The numerical viscosity of entropy stable schemes for systems of conservation laws, I, *Math. Comput.* **49** (1987) 91–103.
[24] E. Tadmor, Entropy stability theory for difference approximations of nonlinear conservation laws and related time-dependent problems, *Acta Numer.* (2004) 451–512.
[25] J. G. Trulio and K. R. Trigger, Numerical solution of one-dimensional hydrodynamical shock problem, UCRL Report 6522 (1961).